A comprehensive review of separator membranes in lithium-ion batteries

Niranjanmurthi Lingappan [a,b,*], Wonoh Lee [b], Stefano Passerini [c,d,e], Michael Pecht [a,**]

[a] Center for Advanced Life Cycle Engineering (CALCE), University of Maryland, College Park, MD, USA
[b] School of Mechanical Engineering, Chonnam National University, 77 Yongbong-ro, Buk-gu, Gwangju, 61186, South Korea
[c] Karlsruhe Institute of Technology (KIT), P.O. Box 3640, 76021, Karlsruhe, Germany
[d] Helmholtz Institute Ulm (HIU), Helmholtzstraße 11, 89081, Ulm, Germany
[e] Department of Chemistry University of Rome "La Sapienza", Piazzale Aldo Moro 5, 00185, Rome, Italy

Keywords:
Lithium-ion batteries
Polyolefin membranes
Nonwoven membranes
Ceramic composite separators
Shutdown functional separators
Fire retardant separators

A B S T R A C T

The widespread adaptation of lithium-ion batteries for consumer products, electrified vehicles and grid storage demands further enhancement in energy density, cycle life, and safety, all of which rely on the structural and physicochemical characteristics of cell components. The separator membrane is a key component in an electrochemical cell that is sandwiched between the positive and negative electrodes to prevent physical contact while permitting ionic conduction through the electrolyte. Though it is an inactive component in a cell, the separator has a profound impact on the ionic transport, performance, cell life, and safety of the batteries. Today there are numerous types of separators in use or being considered, including polyolefin separators, modified polyolefin separators, nonwoven separators, and ceramic composite separators. This review summarizes the state of practice and latest advancements in different classes of separator membranes, reviews the advantages and pitfalls of current separator technology, and outlines challenges in the development of advanced separators for future battery applications.

1. Introduction

Lithium-ion batteries (LIBs) have been the leading power source in consumer electronics and are expected to dominate electric vehicles and grid storage due to their high energy and power densities, high operating voltage, and long cycle life [1]. The deployment of LIBs, however, demands further enhancement in energy density, cycle life, safety, and reduction in cost, all of which rely mainly on the structural and physicochemical characteristics of cell components. Commercial lithium (Li)-ion cells consist of several key components: positive and negative electrodes, metallic current collectors, an organic liquid electrolyte, and a porous polymeric separator. Fig. 1 shows the basic components of a LIB's cell. While these components play a vital role in a cell, the volatile and flammable organic electrolytes and the high oxidation potential of Li-transition-metal-oxide cathodes make LIBs susceptible to fire and explosion [2]. According to the Federal Aviation Administration, there have been numerous battery-related accidents, which are closely related to the failure of cell components [3]. Therefore, a rigorous examination of the physical/chemical characteristics of cell components is of paramount importance to prevent LIB failures.

The separator is a porous polymeric membrane sandwiched between the positive and negative electrodes in a cell, and are meant to prevent physical and electrical contact between the electrodes while permitting ion transport [4]. Although separator is an inactive element of a battery, characteristics of separators such as porosity, pore size, mechanical strength, and thermal stability influence the ion transport, cycle life, performance, and safety of the batteries [5]. Thus, the separator represents one of the key components in LIBs.

Porous separators face multiple challenges in the electrochemical cell, affecting the safety of the cells. The oxidation of metal oxide cathodes and the reduction of the negative electrodes during a charge/discharge processes often lead to the decomposition of organic liquid electrolytes, which can block the pores and affect the separators' function [6]. Further, repetitive charge/discharge processes can lead to lithium dendrite (Li-dendrite) growth, which can penetrate through the separator, leading to physical contact between the electrodes and internal shorting. The occurrence of mechanical/electrical/thermal abuse scenarios during battery operation can physically damage the separators [7,8]. All of these factors induce separator failure, which can eventually lead to battery failure. In extreme cases, these failures may trigger fires or explosions [9]. Designing a separator membrane with ideal

* Corresponding author. Center for Advanced Life Cycle Engineering (CALCE), University of Maryland, College Park, MD, USA.
** Corresponding author.
E-mail addresses: niranjangowri@gmail.com (N. Lingappan), pecht@umd.edu (M. Pecht).

Abbreviation

LIBs	lithium-ion batteries
PE	polyethylene
PP	polypropylene
PTFE	polytetrafluoroethylene
PVDF	polyvinylidene fluoride
PVA	polyvinyl alcohol
PAN	polyacrylonitrile
PET	polyethylene terephthalate
PI	polyimide
PEI	polyetherimide
PEEK	poly (ether ether ketone)
EC	ethylene carbonate
PC	propylene carbonate
DMC	dimethyl carbonate
PMMA	polymethylmethacrylate
PDA	polydopamine
PBI	polybenzimidazole
PMIA	phenylene isophthalamide
BNNT	boron nitride nanotube
ALD	atomic layer deposition

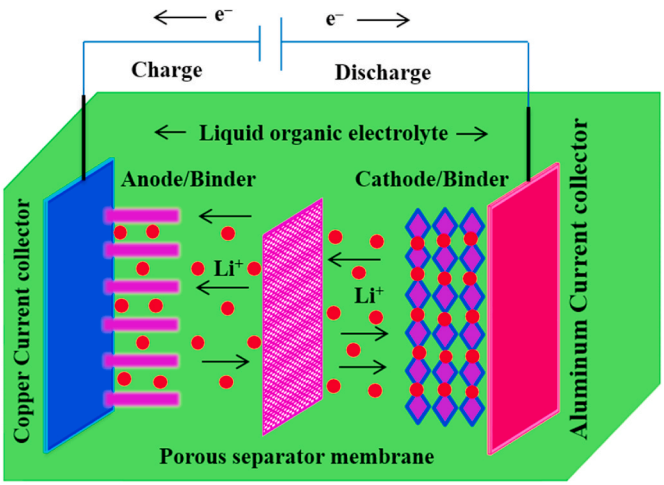

Fig. 1. Schematic illustration of the key components of LIBs.

characteristics is a way to maximize the charge transport kinetics, mitigate separator failures, and prevent premature battery failures.

Arora et al. [10] summarized the fundamental characteristics and manufacturing process of polyolefin separators. Zhang et al. [11] discussed the characteristics and electrochemical performance of separators in association with liquid electrolytes. Waqas et al. [12] described the overview of methodologies that are employed to manufacture numerous separators, including polyolefin separators, nonwoven separators, and ceramic separators. Lee et al. [13] discussed the advancement of polymer and ceramic functionalization of separator membranes and their significance toward the improved Li storage performance. Lagadec et al. [14] described the characterization techniques that are useful to evaluate the characteristics of separator membranes. This review provides a comprehensive overview of the full array of separator membranes that are associated with LIBs. The review starts with an overview of the key properties separators, introduces the different types of separators, and discusses the conditions that induce the failures of separators. Through an assessment on the structure-property relationship and its influence on electrochemical performance, the advantages and disadvantages of the current separator membranes including modified polyolefin, nonwoven, ceramic composites, redox-active, and shutdown functional separators are summarized. Finally, the challenges and perspectives that are important for the development of advanced separator membranes are presented. Fig. 2 shows an overview of the wide range of separators covered in this review.

2. Characteristics of separator membranes

The separator properties must ensure ionic transport, cell life, and the safety of the batteries. The following characteristics that are key to develop separators for LIBs.

2.1. *Chemical stability*

Separators must be chemically and electrochemically inert against the cell components including the electrolyte, active materials, carbon black, and binders subject to reductive and oxidative environments.

2.2. *Thickness*

Separators must be thin but be mechanically strong and flexible enough to withstand stress and strain induced during cell fabrication and operation [13]. The separator thickness for the consumer electronics market is generally set below 25 μm to minimize both cost and size [15]. Thinner separators (<20 μm) have low ionic resistance and high rate capability due to efficient Li ion diffusion; however, they suffer from weak mechanical strength [16]. Thicker separators (>25 μm) show greater mechanical strength, which is essential during cell assembly; however, the thicker separators diminish the ionic transport kinetics, resulting in poorer charge/discharge capacity [17].

2.3. *Porosity*

Porosity is defined as the fraction of the voids within a material, which helps to hold the liquid electrolyte and facilitates efficient Li-ion diffusion between the electrodes. The porosity of the separator depends on the manufacturing process [13]. Separators with large porosity can reduce the internal resistance and facilitate fast ionic transport [18]. For commercial LIBs, the recommended porosity is around 40% [19]. A suboptimal porosity is detrimental to battery life, since the electrolyte intermediates or dendrites can block the small pores, which reduces or even terminates the electrochemical reactions [20]. Porosity beyond the optimal level, however, can reduce tensile strength and degrade the separator during the electrochemical reaction [21]. Further, high porosity makes the separator susceptible to electrical shorts due to the formation of Li-dendrites [13]. Porosity can be measured using the liquid immersion or gas adsorption method.

2.4. *Pore size*

Pores must be smaller than the size of the electrode material particulates and conductive additives. Pores with a uniform size distribution are desirable to ensure homogeneous current distribution. The average pore size of commercial separators is 30–200 nm and less than 1 μm [13]. The large pore size affects the shutdown process since the large pores are impossible to close effectively during shrinkage or melting of the membrane [22]. The pore structure of separators can be analyzed using a capillary flow porosimeter and scanning electron microscopy.

2.5. *Tortuosity*

Tortuosity describes the tortuous state of the pathway within the separator. The tortuous structure of the separators can suppress Li-dendrite growth. However, high tortuosity reduces the effective charge and mass transfer process. The tortuosity of separator can be

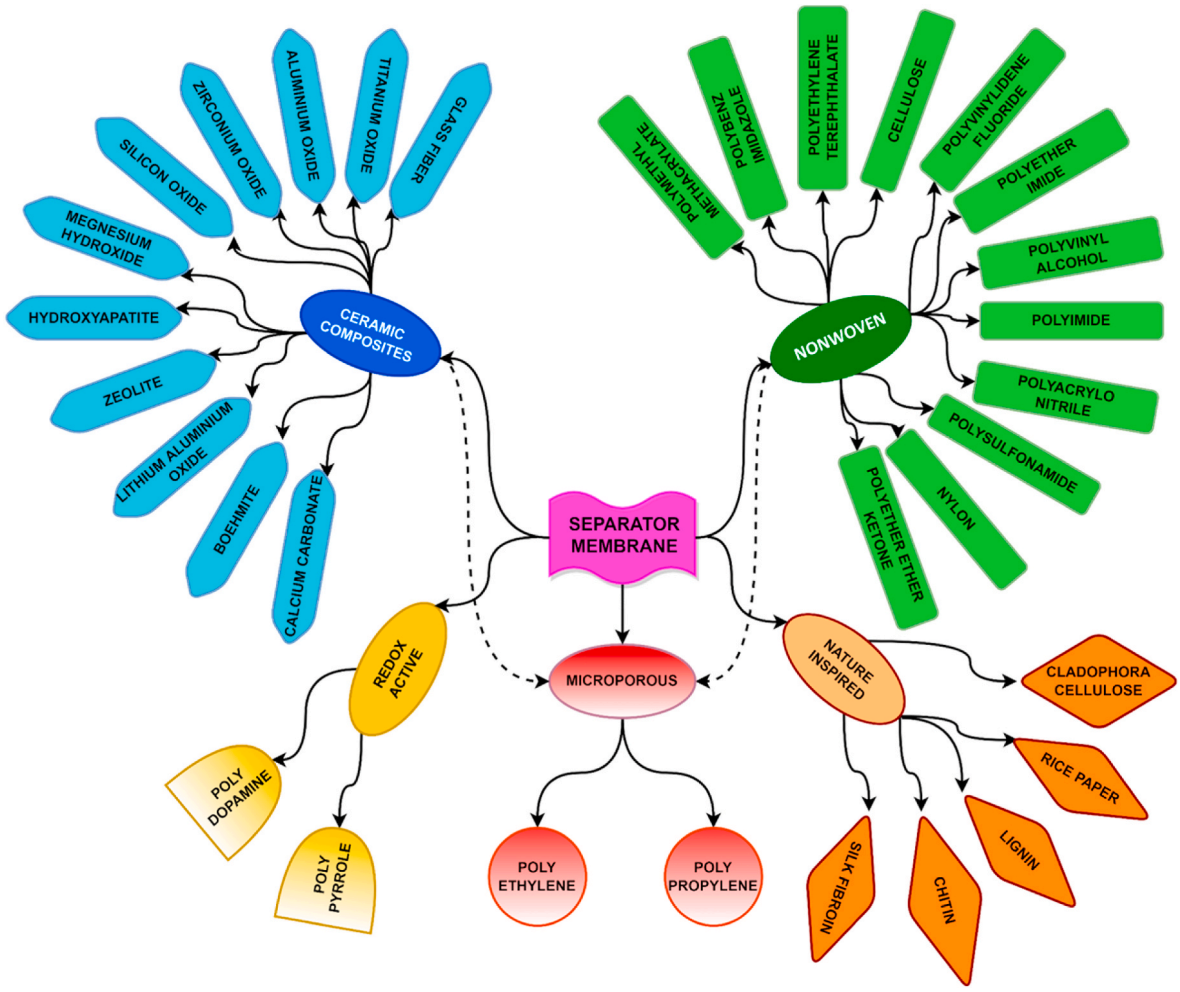

Fig. 2. Overview of separator membranes discussed in the review.

calculated by the following equation [23,24]:

$$Tortuosity = \sqrt{\frac{\varepsilon * \sigma_e}{\sigma_s}} \quad (1)$$

where ε is the porosity and σ_e is the ionic conductivity of electrolyte, and σ_s is the ionic conductivity of the separator.

2.6. Permeability

Permeability is defined as the time required to pass a specific amount of air through a set area of a given separator under a set pressure. It is expressed in terms of a Gurley value. Separators with uniform permeability promote efficient ionic transport between the electrodes. Air permeability is the standard measurement technique employed to measure permeability, and is closely related to the porosity, thickness, pore diameter, and tortuosity of the separators. The microporous single-layer polyolefin separator has Gurley values of around 250–570 s and trilayer polyolefin separator has Gurley values of around 300–600 s [25].

2.7. Mechanical strength

The mechanical properties are characterized in terms of tensile strength along the machine and transverse directions, tear resistance, and puncture strength. Separators must be mechanically strong, especially in the machine direction, and robust enough to withstand the stress induced during battery assembly as well as the continuous charge/discharge process [26]. Tensile strength is a measurement of the force required to pull the separator membrane to the point where is breaks. Tensile strength of 100 MPa has typically been the minimum requirement for commercial applications [27]. Tear resistance is the resistance level of a separator membrane that can withstand the effect of tearing or cracking. Separators with high puncture strength are needed to avoid penetration by particulates in the electrode materials and any needle-like Li-dendrites. Puncture strength is defined as the maximum load required for a given needle to puncture a separator, and it can be measured with a tensile tester. Puncture strength of 300 g has been the typical minimum requirement for commercial applications [27].

2.8. Wettability

High electrolyte affinity/wettability and retention of electrolyte are fundamental requirements for separators to enable homogeneous ionic transport and cycle life of LIBs [28]. The contact angle measurement is used to investigate the wettability of the separator.

2.9. Electrolyte uptake

Electrolyte uptake indicates the amount of liquid electrolyte absorbed by the separator film; it can be calculated from the equation:

$$Electrolyte\ Uptake\ \% = \frac{W_e \quad W_d}{Wd} \times 100 \quad (2)$$

where W_e is the weight of the separator film after immersed in liquid

electrolyte and W_d is the weight of the dry separator before immersed in liquid electrolyte. Electrolyte uptake impacts the ionic conductivity of the cell and, in turn, the specific capacity, rate performance, and cycle life of LIBs. The higher the electrolyte uptake, the higher the electrochemical capacity [29].

2.10. Thermal shrinkage

A separator with low melting temperature tends to melt and shrink, which causes pore blockage and eventually terminates the ion transport between the electrodes [30]. Thus, a separator with a shrinkage of <5% for 60 min at 200 °C has typically been desirable for LIBs [31]. The melt integrity is measured by thermal-mechanical analysis [23].

2.11. Shutdown characteristics

A shutdown function is one of the most important safety aspects of separators. When the cell temperature increases to the melting range of the separators, the micropores of the separator are closed by the melted parts, which blocks the ionic transport pathway between the two electrodes and terminates the electrochemical reactions [32].

2.12. Cost

The separator is one of the most expensive components in LIBs [33]. Choosing cost-effective materials and easy manufacturing process are of vital importance to reduce the cost of separators. The cost breakdown of the separator market is estimated to be 7.7%, as shown in Fig. 3.

3. Classification of separators

Separators are classified into microporous polyolefin separators, nonwoven separators, and ceramic composite separators. The synthesis process and structural characteristics such as porosity, pore-size distribution, thickness, electrolyte affinity, and mechanical properties of these separators differ significantly. The general characteristics of these separators are given in Table 1.

3.1. Microporous polymer separators

Microporous polymer separators represent state-of-the-art separators in commercial LIBs. Polyethylene (PE) or polypropylene (PP) are exemplary candidates in microporous polymer separators. Single-layer PE or PP separators are predominantly employed in commercial LIBs [10]. Fig. 4 shows the scanning electron microscopic image of PE and PP separators, both of which exhibit an open porous structure. The porosity of PE and PP separators is calculated to be around 40% with an average pore size of 50–100 Å. These separators are characterized with various thicknesses ranging from 18 to 25 μm, ionic resistivity of 1.5–2.5 Ω cm^2,

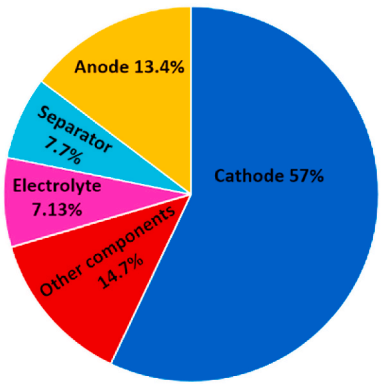

Fig. 3. Cost breakdown of the separators in commercial LIBs.

puncture strength of 300 g/mil, high mechanical strength, and high structural and electrochemical stability [34,35]. Trilayer

(PP/PE/PP) separator is also being used in LIBs [11]. Shutdown function is one of the most prominent aspects of trilayer separators to ensure safety of LIBs [32]. For instance, when the cell temperature becomes close to the melting point of PE (130 °C), the inner PE layer melts down, converting the porous layer into a nonporous structure and thus terminating the ion transport between the electrodes, while the outer PP layer remains stable until the cell temperature reaches the melting temperature of PP (160 °C) [36]. The characteristics of various microporous polyolefin separators are given in Table 1.

Microporous polyolefin-based membranes are manufactured through both dry and wet processes [10]. The dry process involves melting polyolefin resin and extruding it into a film. The resulting film is then thermally annealed to increase the size and amount of the lamella structure and is subsequently stretched into a porous structure [22]. Separator manufacturers such as Celgard LLC and Ube Corp. Ltd. prefer the dry process to prepare PP and PE separators [10]. In the wet process, hydrocarbon liquid is mixed with polyolefin resin and heated to melt the mixture. The resulting melt is extruded into a sheet with an orientation into machine direction and then extracting the liquid with volatile solvent [10]. Separator manufacturers such as Asahi Kasei, Tonen, Mitsui Chemicals, and Entek prefer the wet process to manufacture porous separators [37]. The large-scale production of polyolefin separators by dominant manufacturers and their target applications is given in Table 2.

3.2. Nonwoven separators

Nonwoven separators are fibrous mats, webs, or sheets manufactured from directionally or randomly oriented fibers [38]. The macroporous fibrous matrix is manufactured via a dry laid, melt blown, or wet laid process [12]. The wet laid method is similar to the paper-making process, and the fibers are bonded together by chemical or thermal coupling. The melt blown method is a binder-free process wherein the polymer web fibers are extruded [10]. Electrospinning, an alternate technique, is widely employed to fabricate a wide array of nonwoven membranes such as cellulose [39], polytetrafluoroethylene (PTFE) [40], polyvinylidene fluoride (PVDF) [41], polyvinyl alcohol (PVA) [42], polyacrylonitrile (PAN) [43], polyethylene terephthalate (PET) [44], polyimide (PI) [29], polyetherimide (PEI) [45], and nylon [46]. Some of the nonwoven membranes such as PEI [47] and poly (ether ether ketone) (PEEK) [48], polybenzimidazole (PBI) [49], poly (phenylene isophthalamide) (PMIA) [50], polyphenylene sulfide [51], and polyphenylene oxide [52] are fabricated via the phase inversion method. These separators possess high porosity (up to 80%), high thermal stability (200 °C), and large electrolyte affinity. The general characteristics of nonwoven membranes are given in Table 3.

3.3. Ceramic composite separators

Ceramic composite separators are made up of inorganic particles, either bonded together using a small amount of polymeric binder or coated on polymer or other porous membranes. Various studies examine the ceramic separators such as $CaCO_3$ [53], Al_2O_3 [54], SiO_2 [55], $MgAl_2O_4$ [56], $LiAlO_2$ [57], boehmite [31], ZrO_2 [58], glass fiber [59], and hydroxyapatite [60]. These separators show fibrous structures with high porosity and large surface area. Due to their hydrophilicity, these separators exhibit good wettability in organic electrolytes, especially those containing cyclic carbonates such as ethylene carbonate (EC), propylene carbonate (PC), and butyrolactone with high dielectric constant [53,61]. Moreover, these separators show good dimensional stability even at an elevated temperature (200 °C) [62]. The characteristics of ceramic separators are given in Table 4.

Table 1
The characteristics of microporous polyolefin separators.

Manufacturer	Product name	Materials	Process	Thickness (μm)	Porosity (%)	Pore size (μm)	Gurley number (s)	Melt temp (°C)	Puncture strength (g)
Celgard	Celgard 2730	Single layer PE	Dry	20	43	–	22	135	–
Asahi Kasei	Hipore	Single layer PE	Wet	16	41	–	21	138	–
Asahi Kasei	Hipore	Single layer PE	Wet	25	40	–	21	138	–
Tonen	Setela	Single layer PE	Wet	25	41	–	26	137	–
Entek	Teklon	Ultrahigh molecular weight PE	Wet	13	54	–	–	–	–
DSM	Solupur	Single layer PE	Wet	28	–	0.07	120	132	510
Celgard	Celgard 2400	Single layer PP	Dry	25	41	0.043	620	165	>450
Celgard	Celgard 2500	Single layer PP	Dry	25	55	0.064	200	163	>335
Celgard	Celgard A273	Single layer PP	Dry	16	40	0.039	345	163	>300
Celgard	Celgard 3400/ 3401	Surfactant coated PP	Dry	25	41	0.043	620	–	>450
Celgard	Celgard 3500/ 3501	Surfactant coated PP	Dry	25	55	0.064	200	–	>335
Celgard	Celgard 2340	Trilayer PP/PE/PP	Dry	38	45	0.035	780	135/163	>550
Celgard	Celgard 2325	Trilayer PP/PE/PP	Dry	25	39	0.028	620	135/165	>380
Celgard	Celgard 2320	Trilayer PP/PE/PP	Dry	20	39	530	0.027	135/165	>360
Celgard	Celgard C500	Trilayer PP/PE/PP	Dry	25	35	0.041	515	135/165	>320
Celgard	Celgard C480	Trilayer PP/PE/PP	Dry	21.5	50	0.038	320	135/165	>400
Celgard	Celgard C300	Trilayer PP/PE/PP	Dry	20	36	0.032	560	135/165	>300
Celgard	Celgard C250	Trilayer PP/PE/PP	Dry	18	35	0.032	500	135/165	>300
Celgard	Celgard C200	Trilayer PP/PE/PP	Dry	17	35	0.032	450	135/165	>245
Celgard	Celgard C212	Trilayer PP/PE/PP	Dry	16	35	0.032	435	135/165	>220
Celgard	Celgard M825	Trilayer PP/PE/PP	Dry	16	39	0.026	435	135/165	>300
Celgard	Celgard M824	Trilayer PP/PE/PP	Dry	12	38	0.026	425	135/165	>225

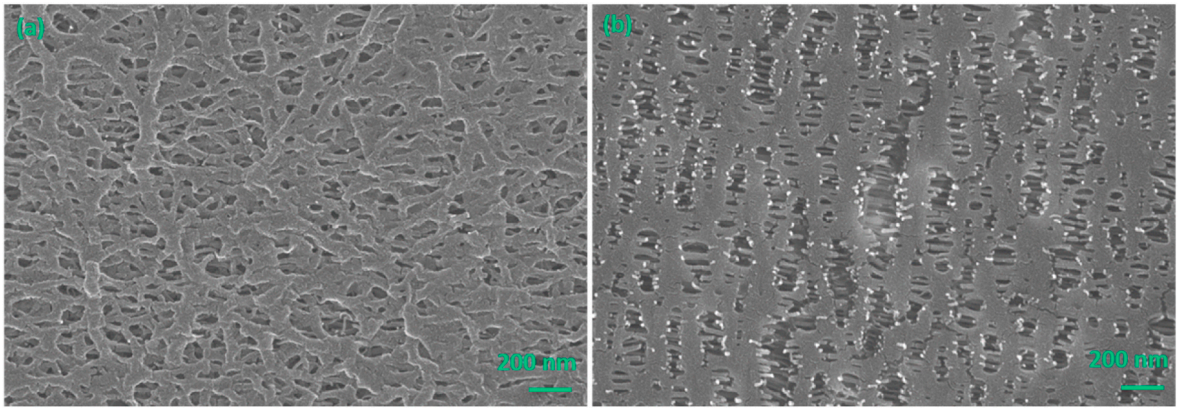

Fig. 4. Scanning electron microscopic image of (a) PE and (b) PP membranes manufactured by Celgard.

4. Separator failure mechanisms

The failure of LIBs is strongly associated with the failures of cell components through structural, chemical, or mechanical failures [63, 64]. The failure of separators is one of the most crucial mechanisms that leads to cell and battery failures. In extreme cases, separator failure may trigger thermal runaway [65]. Separators are designed to perform safely without failing; however, thermal/mechanical/electrical abuse scenarios can induce separator failure [66].

4.1. Physical characteristics of separators

Physical characteristics such as thickness, porosity, electrolyte affinity, and mechanical properties of separators can affect cell performance and battery life. The alignment of separators affects the performance as well as the safety of the cell. Cells comprising separators with nonhomogeneous, wrinkled, or unnoticeably damaged surfaces instantly lead to short circuit [67]. Further, the diameter mismatch between the separator and electrodes—especially in the case of a coin cell—shows a high probability of premature failure due to imperfections at the edges. Separators with wider width provide more repeatable data, whereas the smaller-width samples result in premature failure [26].

4.2. Swelling and softening of separators

A vast number of studies have witnessed that the mechanical properties of dry separators are reduced upon immersing them in electrolyte [68,69]. Separator membranes such as polyolefin and PAN can interact with liquid electrolyte such as dimethyl carbonate (DMC), resulting in softening or swelling of the separator and thereby diminishing the mechanical properties [11]. Immersion of PP separator in organic electrolytes often causes softening up to 50%, resulting in a reduction of Young's modulus (51.8% in the machine direction and 90.3% in the transverse direction) [68,70]. However, the characteristics of PP remain unchanged in polar solvents such as water, PC, and acetonitrile due to strong repulsive interaction [71]. The penetration of DMC molecules into the PP chain resulted in swelling, affecting the mechanical properties of the separators [71].

4.3. Lithium dendrite-induced failure

The charging/discharging process is associated with the formation of

Table 2
The large-scale production of polyolefin separators by leading manufacturers.

Manufacturer	Country	Product name	Type	Material	Process	Target Application
Asahi Kasei Corp.	Japan	HIPORE	Microporous	Polyolefin	Wet	Consumer electronics
Toray Industries Inc	Japan	SETELA	Microporous	Polyolefin	Wet	Consumer electronics, electric vehicles
SK innovations Co. Ltd.	South Korea	CCS	Microporous	Ceramic coated polyethylene	Wet	Consumer electronics, electric vehicles
Celgard LLC	USA	Celgard	Microporous	Polyolefin	Dry	Specialty batteries, Automotive, Consumer electronics
Celgard LLC	USA	CELGARD	Microporous	Ceramic/Polyolefin	Dry	Specialty batteries, Automotive, Consumer electronics
Ube Corporation Ltd.	Japan	UPORE	Microporous	Polyolefin	Dry	Electric vehicles, plug-in hybrid vehicles
Ube Maxwell Kyoto Co. Ltd.	Japan	CPORE	Microporous	Ceramic/polyolefin	Dry	Electric vehicles, plug-in hybrid vehicles
Sumitomo Chemicals Co. Ltd	Japan	PERVIO	Microporous	Aramid/polyolefin	Dry	Electric vehicles
Mitsubishi Chemical Corp.	Japan	SEPALENT	Microporous	Polyolefin	Dry	Electric vehicles
Mitsubishi Plastics Inc.	Japan	SEPALENT	Microporous	Coated polyolefin	Dry	Electric vehicles
Entek International LLC	USA	TEKLON	Microporous	Ultrahigh molecular weight PE	Wet	Consumer electronics
Evonik Industries	Germany	AEROXIDE	Ceramic-based microporous	Al_2O_3/PE	Dry	Electric vehicles
LG Energy Solution	South Korea	SRS	Ceramic-based microporous/ nonwoven	Polyolefin Glass fiber	–	Consumer electronics
Teijin	Japan	LIELSORT	Coated microporous	Aramid coated PE	Wet	Consumer electronics
Shandong Gelon LIB Co. Ltd	China	GELON	Microporous	Ceramic coated polyolefin	Dry	Battery applications
Soteria Battery Innovation Inc	USA	Soteria	Nonwoven	Aramid nanofiber/PET	Electro spinning	E-bikes
Dreamweaver	USA	Silver's 20	Nonwoven	Nanofiber/microfiber	Electro spinning	Electric vehicles Consumer electronics
Cangzhou Mingzhu Plastics Co. Ltd	China	–	Microporous	Ceramic coated polyolefin	Wet	Electric vehicles Consumer electronics
Senior Technology Materials	China	–	Microporous	Ceramic coated polyolefin	Wet	Electric vehicles
Jinhui High Tech Co. Ltd	China	–	Microporous	Polyolefin	Wet	Consumer electronics
Shnagai SEMCORP	China	–	Microporous	Functionalized Polyolefin	Wet	Consumer electronics
SENIOR	China	–	Microporous	Functionalized Polyolefin	Wet/Dry	Consumer electronics

Table 3
The general characteristics of nonwoven separator membranes.

Separator material	Thickness (μm)	Porosity (%)	Ionic conductivity (mS cm ^{1})	Electrolyte uptake (%)	Tensile strength (MPa)	Melt integrity (Temp °C)	Ref
Cellulose	27	65	1.04	280	50	200	[39]
PTFE	NR	70	1.87	320	NR	300	[40]
PVDF	NR	84.1	1.83	400	3.25	161	[41]
PVA	28	62	1.2	230	11.5	180	[42]
PAN	25	54	0.76	174	32	200	[43]
PET	NR	89	2.27	500	12	250	[44]
PI	40	72.4	2.15	250	17.5	180	[29]
PEI	45	84.5	3.41	343.9	14	300	[45]
Nylon 6,6	65	66	2.8	260	18	260	[46]
PEEK	28	70.3	1.57	374	124	250	[48]
PBI	30	81	0.13	328	36.4	200	[49]
PMIA	35	63	1.51	173	10.3	400	[50]
Polyphenylene sulfide	29	73.5	1.69	409	119	280	[51]
Polyphenylene	33	50	1.8	115	NR	200	[52]

Table 4
The general characteristics of ceramic separator membranes.

Separator material	Thickness (μm)	Porosity (%)	Ionic conductivity (mS cm ^{1})	Electrolyte uptake (%)	Mechanical strength (MPa)	Shrinkage Rate at Temp °C	Ref
Al_2O_3	37	68	0.93	–	–	150 °C	[54]
SiO_2	200	45	0.35	140	29.3	–	[55]
Glass fiber	25	59.2	1.22	–	–	180 °C	[59]

tree-like Li-dendrites on the surface of the negative electrode [72]. Li-dendrites could penetrate the solid electrolyte interface layer that formed on the negative electrode and eventually grow further to pierce the separators, causing internal shorting [73,74]. This effect becomes more prominent with the cell operating at a higher temperature, where the elastic stiffness of the separators decreases significantly [75].

4.4. Thermal failure

Thermal shrinkage is one of the major causes of separator-induced battery failure [76]. The commercial polyolefin membranes work efficiently at room temperature. However, when the temperature of the batteries becomes abnormally high due to the exothermic reaction occurring within the cell components [77], the separators begin to melt down (130 °C for PE and 160 °C for PP) [78]. This often leads to closure of the pore structure and eventually blocks the ionic transport between the anode and cathode, terminating the electrochemical reactions. With a further increase in temperature, the separators melt down completely, allowing direct contact between the anode and cathode and causing internal shorting [79]. The entire failure of a separator can trigger a fire or even an explosion.

4.5. Mechanical failure

During the electrochemical reaction, separators face mechanical stress from the cathode/anode due to Li intercalation/deintercalation reactions [80]. Under mechanical abusive scenarios, separators tend to tear or even split into multiple fibers [27]. Although mechanical strength and puncture strength measurements may be sufficient to address the integrity of separators, they do not provide a full understanding of the mechanical failure of the separator membranes. A better understanding of the mechanical failures of separators is required, especially when considering the behavior of the battery under external mechanical loading, such as in the event of a crash [81].

5. Recent advances in separator membranes

State-of-the-art polyolefin separators have been widely employed in commercial LIBs; however, low electrolyte affinity (due to their hydrophobicity) and low melting temperature (130 °C for PE) are major limitations associated with these separators. Although single-layer PP can function up to 160 °C, the electrolyte affinity remains a hurdle. Due to these limitations, there has been a tendency to develop advanced separators for LIBs.

5.1. Trends in polyolefin separators

Modification of conventional polyolefin separators is one of the most prominent strategies to improve electrolyte affinity and thermal properties while maintaining the separator's intrinsic properties.

5.1.1. Surface treatment of polyolefin separators

High-energy radiation approaches such as gamma ray, e-beam radiation, and oxygen plasma treatments were employed to improve the surface properties of separators [82]. The oxygen plasma treatment has improved the inherent porosity and electrolyte affinity of conventional separators due to the formation of oxygen functional groups [83]. The gamma ray and e-beam irradiation approaches have induced cross-linking within the PE backbone, which resulted in enhanced thermal properties [82]. As a result, the surface-treated separator sandwiched Li/$LiMn_2O_4$ cell delivered capacity retention of 85.4% even at 55 °C, whereas the Li/$LiMn_2O_4$ cell comprising pristine separator showed capacity retention of 53.7% under similar conditions [83]. Note that the surface treatment time and radiation dose have showed significant impact on the characteristics of the base separators. The surface treatment beyond optimal time led to the complete destruction of the porous structure, resulting in reduction in ionic conductivity as well as mechanical strength [84]. Further, the high radiation dose has destroyed the inherent porous structure due to the melting of the polymer backbone, diminishing the porosity of the separator [85].

5.1.2. Polymer functionalized polyolefin separators

Polymer functionalization represents one of the prominent approaches to mitigate the inherent drawbacks of polyolefin separators. Various polymer matrices, including polymethylmethacrylate (PMMA) [86], polydopamine (PDA) [87], and cellulose derivatives [88], were coated on the conventional separator through a solution phase dip coating method. Functional polymers such as PMMA [89], polyethylene oxide [90], and polyacrylic acid [91] were covalently coupled to the pristine membrane via atom transfer radical polymerization and radiation-induced techniques. The characteristics and electrochemical performance of the polymer functionalized polyolefin separators are listed in Table 5. Note that the physical and chemical characteristics of the functionalized polymers influenced the properties of the pristine separators. For instance, polymer matrices such as PVDF [92], polysulfonamide [93], and polyampholyte [94] preserved the inherent porosity of the pristine separators owing to their open porous network. As a result, the functionalized separators showed comparable ionic conductivity to that of pristine separators. However, these separators exhibited thermal shrinkage of ~30% at 150 °C due to their low melting point [92]. The functionalization using thermally stable polymers such as PI [95], PBI [96], polyhexavinyldisiloxane [97], poly *m*-phenylene isophthalamide [98], phenylene terephthalamide [99], and phenolic resin [100] showed negligible thermal shrinkage up to 150 °C due to the incorporation of a thermally stable polymer backbone. The polycations functionalization such as polyethyleneimine repelled the migration of dissolved metal cations from cathodes (such as Mn^{2+} ions from Li_2MnO_4 cathode) and thereby prevented the migration of dissolved cations to the negative electrodes [101]. Aramid nanofiber functionalized PE and PP separators displayed high tensile strength and high heat resistance as compared to pristine membranes due to their mechano-thermal properties [102]. The functionalization of polyolefin separators using gel polymer electrolytes such as poly(acrylonitrile-*co*-methyl methacrylate) and polyelectrolytes such as polyethylenimine, polystyrenesulfonate, and poly-L-lysine/polyethylene glycol through a layer-by-layer assembly approach resulted in ultrathin coating (around ~2 nm) on the base separators [103,104]. The ultrathin coating preserved the surface morphology and porosity of the base separators, resulting in ionic conductivity of 2.06 mS cm^{-1} [104]. Note that the grafting degree of polymers affected the characteristics of the separator. Although grafting degree beyond the optimal condition exhibits improved mechanical and thermal properties, the porosity of the separators is reduced, which affects the ionic transfer process [86,89].

In summary, polymer functionalization of polyolefin separator shows great promise in improving surface wettability, electrolyte retention, and thermal stability. Nevertheless, the ability to control the polymer thickness is the most crucial aspect to maintain the inherent porosity and ionic conductivity of the base separators.

5.1.3. Ceramic-coated/deposited polyolefin separators

Ceramic functionalization has been widely investigated to improve the electrolyte affinity and thermal properties of polyolefin separators. A variety of ceramic materials such as Al_2O_3 [105], SiO_2 [106], TiO_2 [107], metal organic framework [108], ZrO_2 [109], boehmite [110], $Al(OH)_3$ [111], and $Mg(OH)_2$ [112] were deposited on the polyolefin separators. Oxide derivatives of metals such as niobium, hafnium, tantalum, lanthanum, and yttrium were deposited on commercial separators [113]. The characteristics and electrochemical performance of various ceramic functionalized polyolefin separators are listed in Table 6. In this approach, ceramic particles were homogenously mixed with polymeric binders and the resulting slurry was then coated on the base separator. In an alternate approach, the base separator was exposed to the ozone or oxidation treatment in order to improve the adhesion with the ceramic layers [113]. The incorporation of ceramic particles partially reduced the pore size and thereby improved the electrolyte retention of the separator. The size of the ceramic nanoparticles showed an impact on the characteristics of the separators [106]. For instance, smaller SiO_2 nanoparticles (40 nm) deposited separator showed porosity of 68%, thermal shrinkage of 23% (at 140 °C), and a uniform ionic

Table 5
The characteristics and electrochemical performance of the modified polyolefin separators.

Separator	Thickness (μm)	Porosity (%)	Ionic conductivity (mS cm ^{1})	Electrolyte uptake (%)	Mechanical strength (MPa)	Gurley number (s)	Shrinkage Rate at Temp (°C)	Cell	Electrolyte	Capacity retention (%)	Ref
PMMA/PE	–	21.4	1.19	183	69.8	157	–	Graphite /$LiFePO_4$	1 M $LiPF_6$/ EC/DMC/ DEC	95% after 110 cycles	[89]
Polysulfonamide/ PP	50	65	0.80	200	–	26	Nil at 150 °C	Graphite/ $LiCoO_2$	1 M $LiPF_6$/ EC/DMC	90% after 60 cycles	[93]
PI/PP	24	40.2	0.35	207.6	137.8	273	Nil at 150 °C	Li/NMC	1 M $LiPF_6$/ EC/DMC/ EMC	79.8% after 200 cycles	[95]
PBI/PE	28	54	0.59	225	–	–	Nil at 140 °C	Li/ $LiFePO_4$	1 M $LiPF_6$/ EC/DMC/ EMC	97.7% after 100 cycles	[96]
Phenolic resin/PE	24	57	0.60	227	105	282	6% at 145 °C	Li/ $LiFePO_4$	1 M $LiPF_6$/ EC/DEC	86% after 450 cycles	[100]

Table 6
The characteristics and electrochemical performance of ceramic functionalized polyolefin separators.

Separator	Thickness (μm)	Porosity (%)	Ionic conductivity (mS cm ^{1})	Electrolyte uptake (%)	Gurley number (s)	Shrinkage Rate at Temp (°C)	Cell	Electrolyte	Capacity retention (%)	Ref
Al_2O_3/PSS/ PE	30	–	0.83	248	–	4.5% at 105 °C	MSCB/ $LiCoO_2$	1 M $LiPF_6$/EC/ DMC	88.1% after 200 cycles	[105]
PE/ZrO_2/	29	57	0.61	120	210	17% at 120 °C	Li/$LiCoO_2$	1 M $LiPF_6$/EC/ EMC	97% after 100 cycles	[109]
$Al(OH)_3$/PE	32	84	1.001	127	352	6.6% at 140 °C	Graphite/ $LiCoO_2$	1.15 M $LiPF_6$/ EC/EMC	63% after 300 cycles	[111]
$Mg(OH)_2$/PE	18.5	–	0.73	103.8	234	Nil at 200 °C	Li/NCM	1.15 M $LiPF_6$/ EC/EMC/DMC	77.8% after 1000 cycles	[112]
SiO_2 aerogel/ PP	31	–	0.63	346	–	Nil at 160 °C	Li/$LiFePO_4$	1 M $LiPF_6$/EC/ DMC	87.4% after 100 cycles	[114]
Zeolite 4A/PP	35	58	2.25	270	–	14.4% at 160 °C	Li/$LiFePO_4$	1 M $LiPF_6$/EC/ DEC/DMC	96.2% after 100 cycles	[115]
PE/Si-oxyborate-Al_2O_3	–	–	0.68	268.7	348.2	Nil at 200 °C	Li/$LiCoO_2$	1 M $LiPF_6$/EC/ EMC/DMC	54.1% after 1000 cycles	[116]
Al_2O_3/PE	23	–	1.12	70	–	2.5% at 145 °C	Graphite/ $LiCoO_2$	–	94.7% after 50 cycles	[117]

transfer process due to the homogeneous distribution of particles over the separators. The larger SiO_2 nanoparticles (530 nm) deposited separator showed porosity of 50% and thermal shrinkage of 67% (at 140 °C). The reduction of porosity by the large particles also affected the charge transfer process [106].

Note that the dimensional structure of the ceramic materials showed influence on the characteristics of the base separators. For instance, the deposition of one-dimensional SiO_2 nanotubes over the base separators resulted in random distribution and partial pore closure, while the SiO_2 spheres were uniformly distributed and blocked the pores of the base separator. Due to the different distribution, the SiO_2 tube/PE separator demonstrated higher ionic conductivity and electrolyte affinity than the SiO_2 sphere/PE separator [118]. Mesoporous SiO_2 aerogel (meso/-macroporous) coated separator displayed negligible thermal shrinkage (up to 160 °C) and large electrolyte affinity (346%) due to the large surface area of SiO_2 aerogel [114]. However, the Li/$LiCoO_2$ cell comprising meso/macroporous SiO_2/PE separator resulted in constant capacity degradation upon cycling (capacity decay of 18% up to 100 cycles), due to the large electrolyte consumption by the meso/-macroporous structure [119]. Besides Al_2O_3 and SiO_2, some of the other ceramic materials displayed interesting properties. For instance, TiO_2 nanoparticle functionalized PE and PP separators showed high electrolyte affinity and flame-retardant properties [120]. Porous zeolite frameworks functionalized PP separator displayed an open porous structure, large electrolyte uptake (270%), and high ionic conductivity (2.25 mS cm ^{1}) due to their large surface area [115]. However, the existence of a porous structure led to the large electrolyte consumption and resulted in constant capacity degradation [121]. Silica-oxygen-borate (Si–O–B) coated Al_2O_3/PE, a ternary separator, manifested a puncture strength of 759.1 gF mm ^{2} and dimensional stability (at 200 °C), owing to the strong Al–O–Si–O bonding interaction. Further, the Si–O–B moiety showed scavenging ability toward HF owing to its Lewis acidic character. Due to these merits, the Li/$LiCoO_2$ cell comprising Si–O–B/Al_2O_3/PE separator exhibited stable cycling performance with the capacity retention of 54.1% and the NMC/graphite cell comprising the separators showed the capacity retention of 42.8% after 1000 cycles (in 1 M $LiPF_6$ in EC/EMC/DMC electrolyte) [116]. The borides of metals/nonmetals coated polyolefin separators exhibited high water absorption capability and thereby reduced the acidic impurity generated by moisture presented in the cell, which prevented electrolyte deterioration. Moreover, the cell comprising the boride coated separators showed heat resistance up to 150 °C due to the separators' high thermal stability [122]. Ceramic hydroxides such as AlOOH, $Al(OH)_3$, and $Mg(OH)_2$ coated PE separators exhibited zero thermal shrinkage at 200 °C. Further, these separators showed flame-retardant properties due to the dehydration behavior ($2AlOOH \rightarrow Al_2O_3 + H_2O$), which is an important safety aspect for future LIBs [110–112].

Optimization of the ceramic content is the most important aspect to achieve intriguing characteristics as well as remarkable electrochemical performance. The ceramic content beyond the optimal level affected the characteristics of the separator due to blockage of pores [123]. Further, high ceramic content required large binder content to facilitate strong binding adhesion. However, the large binder content blocked the pores of the separator, affecting the ionic transfer process. The large binder

content also resulted in significant thermal shrinkage due to the thermal decomposition of the binders [105]. Thickness of the ceramic layer is another parameter that influences the characteristics of the separators. For instance, the Al_2O_3 functionalized PE separator with the Al_2O_3 with the thickness of 9 μm showed dimensional shrinkage of 2.5%, Al_2O_3 with the thickness of 6 μm exhibited the shrinkage of 12.7%, and Al_2O_3 with the thickness of 3 μm displayed dimensional shrinkage of 29.3% at 145 °C [117]. While dry approaches demonstrated acceptable properties owing to the formation of thin ceramic layers, the weak adhesion between the ceramic layer and base substrate was the substantial barrier. As a result, the weakly adhered ceramic layer could be desquamated from the base substrate, leading to capacity degradation. To improve the surface adhesion between the separator and ceramic layer, a covalent coupling strategy was demonstrated, which utilized silane analogues as a coupling agent [124]. Coating both sides of the separator is an important aspect to minimize the thermal shrinkage of base separators. For instance, boron nitride nanotube (BNNT) functionalized both sides of the PP separator (BNNT/PP/BNNT) manifested high thermal stability at 150 °C, whereas the BNNT coated on a single side of PP (BNNT/PP) separator showed severe thermal shrinkage at 150 °C. Due to its high thermal stability, the Li/$LiFePO_4$ cell comprising BNNT/PP/BNNT separator functioned up to 70 °C, while the BNNT/PP operated only at 50 °C, and the pristine PP did not function at 50 °C [125]. Nevertheless, coating on both sides can reduce the porosity and diminish the ionic diffusion process.

Characteristics of polymeric binders influence the properties of the separators. Various binders such as poly(lithium 4-styrenesulfonate) [105], carboxymethyl cellulose/styrene butadiene [117], PVA [126], poly(acrylonitrile-*co*-methacrylate) [123], and PVDF [127] were employed to prepare ceramic layers. Due to high elasticity and the presence of hydroxyl and carboxyl groups, carboxymethyl cellulose/styrene butadiene binder showed better adhesive properties as compared to other binders [117]. However, ceramic functionalized separators comprising these binders exhibited significant thermal shrinkage, which stems not only from the base separators but also from the decomposition of these binders [127]. Notably, ceramic functionalized separators comprising thermally stable polymeric binders such as PI [128], polyurethane [112], polyetherketone [129], and cellulose diacetate [130] exhibited zero dimensional shrinkage even at 200 °C. Besides the characteristics of binders, content of the binders also affected the properties of separators. Binders with large content and high molecular weight substantially blocked the pores of the separator and thus reduced the ionic transport kinetics, which were verified by large Gurley value [105,126,130]. Thus, binders that exhibit high adhesive property—even with small content—are required to maintain the inherent porosity of the separators.

Ceramic functionalization is performed mainly through a dip coating process. Using this approach, various ceramic layers were coated on the base separators [106,109,116,123,131]. Although this method is easy, controlling the layer thickness is a tedious task [106,123]. Ceramic functionalization through dry approaches such as radio frequency sputtering [132], atomic layer deposition (ALD) [133], physical vapor deposition [134], and chemical vapor deposition [135] were performed. Prior to the ceramic deposition, surface treatment such as oxygen plasma was performed on the bare polyolefin to strengthen the adhesion between the ceramic layer and bare separator [107,135,136]. Due to the formation of oxygen-functional groups, the hydrophilicity of the separators increased, resulting in conformal coating on the base separator [107,136]. Among various dry approaches, ALD has been widely employed owing to the precise ceramic layer thickness and small environmental impact without involving chlorinated solvents. This technique guaranteed the formation of a thin ceramic layer (up to ~6 nm) over the substrate, which can preserve the porosity and pore structure of the bare separator [137]. A wide range of ceramic oxides such as Al_2O_3, SiO_2, TiO_2, and zinc oxide with thickness ranging from 20 to 100 nm were deposited on polyolefin separators through the ALD method [138]. Note that the ALD cycle numbers showed strong impact on the characteristics of the separator [139]. For instance, Al_2O_3/PP derived from the 50 cycles led to the formation of an Al_2O_3 layer with a thickness of 6 nm, which preserved the inherent porosity of the PP separator. ALD for 100 cycles led to the formation of an Al_2O_3 layer with the thickness of 12 nm, which reduced the porosity of PP from 55% to 26%. Although the porosity is markedly reduced, the Al_2O_3/PP showed negligible thermal shrinkage up to 160 °C, whereas Al_2O_3/PP (50 cycles) showed shrinkage of 24% and bare PP showed shrinkage of 50% at 160 °C [140].

In summary, incorporation of ceramic layers significantly improved the electrolyte affinity and ionic conductivity of the polyolefin separators; however, some of the ceramic materials such as TiO_2, ZrO_2, and the metal organic framework incorporated polyolefin separators still exhibited thermal shrinkage, even at 150 °C. Choosing an ideal binder with high adhesive property and high thermal stability is crucial to achieve separators with high dimensional stability. The ceramic deposition beyond optimal content can result in severe blockage of pores and impede ionic transport between the electrodes.

5.1.4. Ceramic-polymer functionalized polyolefin separators (ternary hybrid)

One of the substantial challenges of ceramic/polyolefin separators is the weak interaction between the ceramic particles and the base separator. Under any abuse scenarios, the dispersed ceramic particles can be desquamated from the hydrophobic separator. To mitigate this issue, ceramic nanoparticles were coated on the polymer functionalized separator. Various polymers such as PDA [141], poly 3,4-ethylenedioxythiophene-*co* polyethylene glycol [142], PEI [143], PDA/PEI [144], PMMA [145], and polyacrylic acid [146] were used as an interfacial layer to facilitate the strong coupling interaction between the ceramic layer and base separator. In an alternate method, the PDA was coated on the SiO_2 deposited PE separator to prevent the delamination of the ceramic layer from the base separators [147]. As a result, the ternary separator (PDA/SiO_2/PE) preserved the dimensional stability, even at 200 °C. In an alternate appraoch, an insulating ceramic layer and microporous polymer layer were sequentially deposited on PE or PP base separators, and the resulting separator showed negligible shrinkage, even at 200 °C. The inclusion of a microporous polymer layer induced pore closure during overheating, ensuring the safety of the batteries [148].

The ternary separator comprising polyolefin separator, ceramic particles, and a polymer layer presents a promising approach to mitigate delamination issues. Nevertheless, the optimization of ceramic content and control over polymer thickness are the key aspects to preserve the porosity and pore size of the base separators.

5.2. Nonwoven membrane separators

Nonwoven separators were widely investigated in LIBs owing to their open porous structure, large electrolyte affinity, and high thermal stability. The nonwoven separators were functionalized with various polymer matrices and ceramic materials to reduce the porosity and large pore size.

5.2.1. Cellulose-based separators

Cellulose nonwoven separators showed ultimate thickness (25 μm), large electrolyte uptake (340%), high ionic conductivity (1.75 mS cm^{-1}), and outstanding thermal stability (up to 200 °C) [149–152]. The high electrolyte affinity of the cellulose-based nonwoven membranes was attributed to the strong interaction between the electrolyte molecules and abundant oxygen functional groups on a cellulose backbone [153]. Nevertheless, high porosity (75%) and large pore size (>2 μm) were the major limitations that may induce physical contact between electrodes and cause internal shorting [39]. To alleviate these limitations, a variety of polymers such as PVDF [39,154], polysulfonamide [155], PDA [156], and styrene-co-acrylate [157] were coated on the

cellulose separator. The overall characteristics and electrochemical performance of the cellulose-based nonwoven membranes are given in Table 7. After functionalization, the inherent mechanical strength and electrolyte affinity of the cellulose separators were remarkably improved. For instance, the chemically cross-linked cellulose/PI membrane displayed the tensile strength of 34.2 MPa, which is nearly five times larger than the pristine PI and electrochemical stability window up to 5.1 V [158]. Attapulgite clay and ammonium polyphosphate functionalized bacterial cellulose membrane exhibited flame-retardant properties [159,160]. Various ceramic materials such as Al_2O_3 [161], SiO_2 [162], and halloysite nanotube [163] were incorporated onto the cellulose membrane. The ceramic dispersed cellulose separators exhibited high ionic conductivity (5.13 mS cm ^{1}) and electrolyte affinity of 625%. Despite their intriguing properties, the polymers and ceramic materials functionalized separators show high porosity (<70%) and large pore size (~3 μm), which are not favorable characteristics for commercial applications [157,161,162]. More importantly, the presence of abundant oxygen functionalities can react with Li^+ ions, resulting in poor reversibility and capacity decay.

5.2.2. Fluorine-containing polymeric separators

Fluorine-containing polymers such as polytetrafluoroethylene (PTFE) and PVDF were employed as binders and as skeletons for gel polymer electrolytes in LIBs [64]. In addition, fluorine-containing polymers have also been employed as separators in LIBs. The PTFE membrane fabricated through an electrospinning approach displayed an open porous structure, good ionic conductance, and high mechanical strength [164]. Nevertheless, the PTFE membrane showed poor electrolyte affinity due to its hydrophobicity, affecting the electrolyte affinity. More importantly, the high melting point of the PTFE (300 °C) membrane affects shutdown function, posing a severe safety risk [40]. The PVDF membrane, an exemplary candidate in fluorine-containing polymers, exhibited open porous structure, high ionic conductance, large electrolyte affinity, and shutdown function at 150 °C [41]. To further improve the electrolyte affinity and thermal properties, various functional polymers—including PTFE, PDA, and cellulose—were incorporated into PVDF membranes [165,166,177]. The overall characteristics and electrochemical performance of the PVDF-based nonwoven membranes are given in Table 7. These functional polymers reduced the high porosity and large pore size and improved the thermal shrinkage up to 170 °C [166]. A variety of ceramic particles, including SiO_2 [20], Sb_2O_3 [167], montmorillonite [168], zeolite [169], halloysite nanotube [178], and layered double hydroxide nanosheets [179], were incorporated on the PVDF membrane via electrospinning, phase inversion, and dip-coating processes. Due to the improved thermal property, the $LiFePO_4$/Li cell comprising Al_2O_3 incorporated PVDF membrane demonstrated stable cycling profile with the capacity retention of 87.5% after 500 cycles at an elevated temperature of 80 °C [180]. The ceramic dispersed PVDF separators manifested high electrolyte affinity (up to 646%); however, porosity and pore size were still remarkably high, which affects the safety of LIBs. Further, the gel formation or even complete dissolution of PVDF in organic electrolytes such as PC is a major concern associated with PVDF-based separators.

5.2.3. Polyvinyl alcohol (PVA) separators

PVA membrane separators were manufactured through an electrospinning approach, and the resulting separator membrane demonstrated porosity of 60% and high electrochemical stability up to 5.0 V [42]. The PVA membrane showed high electrolyte affinity (170%) due to the presence of hydroxyl groups. The cellulose functionalized PVA fabricated through the phase-inversion method displayed negligible thermal shrinkage, even at 200 °C, and a high Li^+ ion transference number (0.54) [181,182]. A zirconium-based metal organic framework was covalently coupled to the PVA separator through an electrospinning approach. The strongly coupled separator showed the ionic conductivity of 2.9 mS cm ^{1}, electrolyte uptake of 230%, and dimensional stability at 200 °C [183]. Impressively, the metal organic framework/PVA separator sandwiched NCM/graphite cell containing 1 M $LiPF_6$ in EC/DEC electrolyte delivered a capacity retention of 73% after 1000 cycles. Nevertheless, the large surface area of the metal organic framework/PVA membrane (1140 m^2 g ^{1}) could be a detrimental factor, accelerating the constant capacity degradation [183]. The overall characteristics and electrochemical performance of the PVA-based nonwoven membranes are given in Table 7.

5.2.4. Polyacrylonitrile (PAN) separators

PAN nonwoven membranes were fabricated through an electrospinning approach, and the resulting membrane exhibited a thickness of 25 μm, pore size of 0.25 μm, and porosity of 60%; these membranes are also low cost, showing great potential as separators in LIBs [43,184]. Because of its high thermal stability (200 °C), the PAN nonwoven membrane remained stable during the hot oven test conducted at 130 °C [43]. Further, the Li/NMC cell comprising the PAN membrane exhibited a lower self-exothermic reaction rate (0.78 °C min ^{1}) than the PE separator (159 °C min ^{1}), verifying the safety of the cell [184]. The PAN separator showed high affinity in electrolytes with high dielectric constants such as EC, PC, and DMC and also with ionic liquid electrolytes [185]. The organic and polymeric materials such as lignin and polysulfonamide functionalized PAN separator exhibited thermal stability up to 180 °C [186,170]. The dihydro phosphaphenathrene oxide functionalized PAN showed ionic conductivity of 6.49 mS cm ^{1}, which is the best ionic conductivity reported for PAN as well as other nonwoven-based separators. Further, the dihydro phosphaphenathrene moiety reduced the thermal stability of the PAN base material from 250 °C to 130 °C, indicating that the dihydro phosphaphenathrene moiety promptly shut down the battery [187]. A gel polymer electrolyte based on a PAN/PVA blending membrane displayed electrolyte affinity of 585%, thermal stability up to 160 °C, and a wide electrochemical stability window exceeding 5.2 V (in 1 M $LiPF_6$ in EC/DMC/EMC electrolyte). With these key merits, the Li/$LiCoO_2$ cell comprising PAN/PVA gel polymer membrane exhibited stable cycling performance with the capacity retention of 96% after 200 cycles [188]. Mussel-inspired functionalization of PAN demonstrated high heat resistance, an electrochemical stability window of ~5.25 V, and fire-retardant properties [189,190]. Notably, the PDA/PAN membrane displayed stable voltage performance with a small overpotential (10 mV) for 700 h [171]. The ceramic materials such as SiO_2 [172], Al_2O_3 [191], and lithium lanthanum titanate [192] functionalized PAN separators exhibited high ionic conductivity, high thermal stability, and electrochemical oxidation stability (up to 5.7 V). The overall characteristics and electrochemical performance of the PAN-based nonwoven membranes are given in Table 7.

5.2.5. Polyethylene terephthalate (PET) separators

The PET nonwoven membranes are of great interest owing to their good structural and mechano-thermal properties. The fibrous PET membrane fabricated through an electrospinning method displayed porosity of 40%, ionic conductivity of 2.27 mS cm ^{1}, and large electrolyte uptake of 500% [44]. Despite these merits, large pore size (~2 μm) is the major concern that may induce internal shorting. To circumvent this issue, polymeric materials such as PMMA [193], PVDF [194], and PI [195] were incorporated into the PET separator, and the resulting separators showed moderate pore size (~1 μm) and thermal shrinkage of 2% at 180 °C. The ceramic particles such as SiO_2 [196] and Al_2O_3 [197] were incorporated into the PET-based separators, and the resulting separators showed pore size of 1 μm and thermal stability up to 200 °C. Overall, PET-based separators exhibit impressive thermal properties and shutdown capability (130 °C) [198]. The ceramic functionalized PET separators are currently under the large-scale production for commercial applications. The characteristics and electrochemical performance of the PET-based nonwoven membranes are given in Table 7.

Table 7
The characteristics and electrochemical performance of different polymer matrices and ceramic materials functionalized nonwoven membranes.

Separator material	Thickness (μm)	Porosity (%)	Ionic conductivity (mS cm^{-1})	Electrolyte uptake (%)	Mechanical strength (MPa)	Shrinkage Rate at (Temp °C)	Cell	Electrolyte	Capacity retention (%)	Ref
Cellulose/PVDF	27	65	1.04	280	50	Nil at 200 °C	Graphite /$LiCoO_2$	1 M $LiPF_6$/EC/DMC	83% after 100 cycles	[39]
Cellulose/PSA	40	66	1.2	260	–	Nil at 200 °C	Graphite /$LiCoO_2$	1 M $LiPF_6$/EC/DMC	85% after 100 cycles	[155]
Cellulose/PDA	40	62	0.95	200	21	Nil at 200 °C	Graphite /$LiCoO_2$	1 M $LiPF_6$/EC/DMC	84.9% after 100 cycles	[156]
Cellulose/Al_2O_3	30	74.7	4.91	625	140	Nil at 180 °C	Li/$LiFePO_4$	1 M $LiPF_6$/EC/DEC/ DMC	89% after 50 cycles	[161]
Cellulose/SiO_2	–	75	1.54	250	14.3	Nil at 200 °C	Li/$LiFePO_4$	1 M $LiPF_6$/EC/DEC	98% after 100 cycles	[162]
Cellulose/Halloysite	30	83	5.13	369	84.4	Nil at 180 °C	Li/$LiFePO_4$	1 M $LiPF_6$/EC/DMC/ DEC	95% after 100 cycles	[163]
PTFE/PDA/SiO_2	–	56	1.33	242	–	Nil at 300 °C	Li/$LiFePO_4$	1 M $LiPF_6$/EC/DEC	89.8% after 200 cycles	[164]
PVDF/PDA	–	85	0.96	1160	–	Nil at 150 °C	Li/ $LiMn_2O_4$	1 M $LiPF_6$/EC/DMC	95.8% after 200 cycles	[165]
PVDF/Cellulose	49	60.2	1.26	370	14.3	Nil at 200 °C	Li/$LiCoO_2$	1 M $LiPF_6$/EC/DMC/ DEC	~99% after 50 cycles	[166]
PVDF/SiO_2	83	85	0.74	646	–	Nil at 160 °C	Li/$LiFePO_4$	1 M $LiPF_6$/EC/DEC	99% after 50 cycles	[20]
PVDF/Sb_2O_3	42	72	2.88	356	–	Nil at 160 °C	Li/$LiFePO_4$	1 M $LiPF_6$/EC/DEC	99% after 100 cycles	[167]
PVDF/ Montmorillonite	58	84	4.20	333	2.39	Nil at 150 °C	Li/$LiFePO_4$	1 M $LiPF_6$/EC/EMC/ DEC	99% after 150 cycles	[168]
PVDF/Zeolite/ PMMA/	–	80	1.72	378	3.2	Nil at 150 °C	Li/$LiFePO_4$	1 M $LiPF_6$/EC/EMC/ DEC	93.8% after 200 cycles	[169]
PAN/PSA	20	87.7	0.24	921	15	Nil at 180 °C	Li/$LiFePO_4$	1 M $LiPF_6$/EC/DMC	90.5% after 70 cycles	[170]
PAN/PDA	50	83.3	1.39	341	13.9	Nil at 200 °C	Li/$LiFePO_4$	1 M $LiPF_6$/EC/DMC/ EMC	66.8% after 105 cycles	[171]
PAN/SiO_2	–	72	3.6	310	–	–	Li/$LiFePO_4$	1 M $LiPF_6$/EC/EMC	99% after 50 cycles	[172]
PI/PEO	80	90	3.83	170	–	Nil at 350 °C	Li/$LiFePO_4$	1 M $LiPF_6$/EC/DMC	96.4% after 100 cycles	[173]
PI/SiO_2	20	90	2.27	2400	–	Nil at 250 °C	Li/ $LiMn_2O_4$	1 M $LiPF_6$/EC/DEC	99% after 100 cycles	[174]
PEI/PVDF	35	64.6	1.38	235	12.1	5% at 180 °C	Li/$LiFePO_4$	1 M $LiPF_6$/EC/DMC/ EMC	99% after 75 cycles	[175]
Fluorinated PEEK	25	88	3.12	559	27.7	Nil at 150 °C	Li/$LiFePO_4$	1 M $LiPF_6$/EC/DMC/ EMC	93% after 300 cycles	[176]

.

5.2.6. Polyimide (PI) separators

The PI nonwoven membranes were fabricated through an electrospinning approach, and the resulting membrane exhibited porosity of 72%, ionic conductivity of 2.15 mS cm ^{1}, and thermal stability up to 180 °C, showing potential as a separator for LIBs [29,199]. Because of its high dimensional stability, a Li/$LiFePO_4$ cell comprising PI separator displayed stable charge/discharge behavior, even at 140 °C [200,201]. A cross-linking PI membrane showed mechanical strength of 90 MPa and flame-retardant properties [202,203]. Various polymer matrices and ceramic materials were incorporated into the PI-based separator, and the functionalized separator exhibited intriguing characteristics. The characteristics and electrochemical performance of the PI-based nonwoven membranes are given in Table 7. For instance, PEG functionalized and fluorinated PI separators showed flame-retardant properties due to the fire extinguishing property of PEG and trifluoromethyl groups [204,205]. The polyethylene oxide functionalized PI separator displayed ionic conductivity of 3.83 mS cm ^{1} owing to the efficient ionic conduction of the polyethylene oxide gel matrix. As a result, the Li/$LiFePO_4$ cell comprising polyethylene oxide/PI separator recovered 75% of its initial capacity at 10C even at 0 °C, while the PI separator showed a rate performance of 53.3% and Celgard 2400 separator showed a rate performance of 3.8%, under similar conditions [173]. The PI/PBI core/sheath nanofiber membrane was fabricated through a combined electrospinning and dip coating process, and the core/sheath membrane exhibited superior thermal stability with zero shrinkage at 300 °C. Because of the high dimensional stability, the Li/$LiFePO_4$ cell comprising PI/PBI membrane demonstrated a stable cycling profile, even at 120 °C. However, the ionic conductivity of the PI/PBI membrane was remarkably low (0.17 mS cm ^{1}) [206]. SiO_2 dispersed PI membrane sandwiched Li/$LiMn_2O_4$ cell displayed good cycling performance with the capacity retention of 99.1% after 100 cycles, even at 55 °C [174]. The remarkable performance was linked to the existence of the SiO_2 layers, which captured the detrimental water and HF in the electrolyte and thereby suppressed the Mn dissolution from the $LiMn_2O_4$ based cathodes at an elevated temperature [207]. The Al_2O_3/PI membrane sandwiched cell displayed a stable OCV profile (4.2 V) during the hot oven test conducted at 160 °C, while the voltage profile of commercial separators reduced instantly [208]. The TiO_2 reinforced PI separator showed fire-retardant properties and stable cycle performance for the Li/$LiFePO_4$ cell (99% after 100 cycles in 1 M $LiPF_6$ in EC/DEC/DMC electrolyte) even at (120 °C) [209]. The ZrO_2 functionalized PI membrane displayed dimensional stability up to 300 °C and stable electrochemical performance, even at an elevated temperature [210]. The silicon nitride (Si_3N_4)-coated PI showed a much lower heat release rate (HRR) (97 W g ^{1}) than the commercial Celgard separator (1142 W g ^{1}). The low HRR value could delay the rate of combustion during a fire accident, which is an important safety aspect of the separators [211].

5.2.7. Polyetherimide (PEI) separators

The PEI membrane showed porosity of 78%, low Gurley value (34 s), thermal stability up to 180 °C, and inherent flame resistance [45,212]. To improve the surface properties, the PEI membrane was functionalized with other polymeric materials and the resulting separators exhibited high electrolyte affinity (306%) [175]. *Para*-phenylenediamine functionalized PEI membrane showed high thermal stability (up to 220 °C) and remained stable after being soaked in 1 M $LiPF_6$ in EC/DMC/DEC electrolyte for 21 days at 55 °C. As a result, the graphite/NMC pouch cell comprising functionalized separator displayed stable cycling performance with capacity retention of 89% even after 1000 cycles [213]. The halloysite nanotube incorporated PEI membrane displayed high ionic conductivity of 5.3 mS cm ^{1} [214]. A ternary membrane based on the SiO_2/PEI/polyurethane showed the highest ionic conductivity (6.25 mS cm ^{1}) [215]. Despite their high ionic conductivity, the large pore size (2 μm) and weak mechanical properties are major drawbacks of the PEI-based separators. The characteristics and electrochemical performance of the PEI-based nonwoven membranes are given in Table 7.

5.2.8. Nylon 6,6 separators

Nylon 6,6, a type of polyamide membrane, was fabricated through an electrospinning approach. The resulting separator exhibited porosity of 67%, ionic conductivity of 2.80 mS cm ^{1}, and dimensional stability up to 150 °C [46]. The SiO_2 nanoparticles dispersed nylon membrane showed good compatibility with different cathode materials such as $LiCoO_2$ (capacity retention of 93% after 50 cycles in 1 M $LiPF_6$ in EC/EMC electrolyte) and $LiFePO_4$ (capacity retention of 98% after 100 cycles in 1 M $LiPF_6$ in EC/EMC electrolyte) [46]. More research efforts on nylon membranes are necessary to understand their potential as separators in LIBs.

5.2.9. Polyether ether ketone (PEEK) separators

The PEEK membrane separators were investigated due to their porosity of 88%, ionic conductivity of 2.80 mS cm ^{1}, and electrolyte affinity of 524% [216]. The highly porous PEEK membrane exhibited a wide electrochemical stability window up to 5.5 V [217]. The ultra-strong PEEK membrane fabricated through the phase inversion method displayed zero shrinkage at 300 °C, high tensile strength (124 MPa), and flame-retardant properties due to a high limiting oxygen index (37%) [218]. The fluorinated PEEK membranes displayed an electrolyte affinity of 559%, ionic conductivity of 3.12 mS cm ^{1}, and thermal stability up to 150 °C. The Li/$LiFePO_4$ cell comprising fluorinated PEEK showed stable cycling performance with capacity retention of 85.4% after 300 cycles (in 1 M $LiPF_6$ in EC/EMC/DMC electrolyte) at 60 °C [176]. Polyarylene ether ketone, a derivative of PEEK, exhibited high thermal stability up to 200 °C [219]. Despite these advancements, the large pore size (2 μm) remains a challenge for further development.

5.2.10. Polymethylmethacrylate (PMMA) separators

The PMMA-based membranes were investigated as separators in LIBs owing to their high ionic conductivity and high electrolyte uptake [220]. Nevertheless, low thermal stability (160 °C) impeded their large-scale application. Although polymers and ceramic materials were incorporated into the base PMMA separator, the resulting separators still exhibited significant thermal shrinkage (29.6%), even at 140 °C [220, 221].

5.2.11. Polybenzimidazole (PBI) separators

The porous PBI membrane exhibited porosity of 81%, electrolyte uptake of 328%, and flame-retardant properties [49]. Due to their thermal and chemical stability, the Li/$LiFePO_4$ cell comprising PBI membrane showed good cycling performance with negligible capacity decay up to 100 cycles, even at 55 °C (in 1 M $LiPF_6$ in EC/EMC/DMC electrolyte) [49,222]. Further, a porous PBI separator sandwiched Li/$LiFePO_4$ cell delivered excellent capacity retention with the recovery of 92.1% of initial capacity after 1000 cycles [223]. Nevertheless, large pore size (2 μm), low mechanical properties, and absence of shutdown functionality limit their feasibility as separators for future LIBs.

5.2.12. Poly(para-phenylene benzobisoxazole) separators

A porous poly(*para*-phenylene benzobisoxazole) membrane was employed as separator in LIBs due to its outstanding mechanical strength (525 MPa) and high shear modulus (6.7 GPa) [224]. It is theoretically predicted that a separator with such a high shear modulus (7 GPa) could effectively suppress Li-dendrite growth [225]. The Li-based cells comprising poly(*para*-phenylene benzobisoxazole) separator displayed steady voltage profile (0.025 V) for 700 h, suggesting the effective suppression of Li-dendrites [224]. The Li/$LiCoO_2$ cell comprising a poly(*para*-phenylene benzobisoxazole) separator exhibited capacity retention of 85.7% after 65 cycles, even at 150 °C [224]. More research endeavors on poly(*para*-phenylene benzobisoxazole) based separators are necessary to understand their effectiveness as separators in LIBs.

5.2.13. Poly (m-phenyleneisothalamide) (PMIA) separators

The electrospun PMIA membrane showed high porosity (60%), high thermal stability up to 400 °C, and electrical insulation capability [50, 226]. The fluorine doping of PMIA improved the electrochemical stability from 4.7 to 5.7 V [227]. The core-shell structure based on a polyurethane/PMIA structure exhibited flame extinguishing properties [228]. The incorporation of SiO_2 layers further improved the electrolyte affinity and ionic conductivity of the pristine PMIA [229]. Nevertheless, the inferior mechanical properties (18 MPa) and shutdown function (180 °C) are not conducive to develop long-term and safe batteries [228].

5.2.14. Polyphenylene sulfide separators

The polyphenylene sulfide separators were employed in LIBs owing to their high thermal stability and large lithium transfer number (0.57) [51]. Glass fiber functionalized polyphenylene sulfide membrane exhibited high thermal stability and flame retardant properties, which are a prerequisite for developing safe LIBs [230]. The ceramic materials such as SiO_2 and polymers such as aramid nanofiber and cellulose functionalized polyphenylene sulfide membrane showed electrolyte uptake around 230%, thermal stability up to 250 °C, and flame-retardant properties [231–233]. The weak mechanical property of the functionalized polyphenylene sulfide (20.5 MPa) is a key limitation of the polyphenylene sulfide-based membranes [232].

5.2.15. Polyphenylene oxide separators

Polyphenylene oxide was employed as a separator owing to its high electrolyte wetting, thermal stability (up to 200 °C), and flame-retardant properties [234]. The SiO_2 incorporated polyphenylene oxide chain displayed zero thermal shrinkage, even at 260 °C [235]. However, the poor ionic conductivity is the major obstacle that hinders further applications.

5.2.16. Polysulfone

Polysulfones and their copolymers were employed as separators in LIBs due to their high thermal stability, chemical resistance, high electrolyte affinity, and high mechanical strength. The polysulfone/PEG copolymer membrane exhibited low thermal shrinkage (2.5%) at a high temperature of 150 °C [236]. The cross-linked microporous polysulfone membrane tends to swell instead of dissolving in the electrolyte during high temperature operation, which ensures the safety of the battery against overheating and fire. Due to the microporous feature, the swelling occurred within the pores of the membrane, maintaining bulk volume of the separator [237].

5.2.17. Polylactide

Polylactide was employed as a membrane separator for LIBs owing to its heat resistance and good electrolyte affinity. The biodegradable property of polylactide makes it easier for recycling after use, which is one of the key merits of polylactide-based separators [238]. Various biocompatible membranes comprising polylactide/cellulose derivatives were prepared via coaxial electrospinning and spin-coating approaches, and the resulting membranes demonstrated improved electrolyte affinity and high thermal stability up to 170 °C [239,240].

5.3. Ceramic composite separators

Ceramic separators based on SiO_2, Al_2O_3, $CaCO_3$, $MgAl_2O_4$, $LiAlO_2$, boehmite, montmorillonite, and ZrO_2 were examined [31,53,56–58, 241]. Because of their brittleness, inorganic separators could be easily broken during the cell winding and assembly process. Thus, a small amount of polymeric binder was used to improve binding strength between particles and flexibility [56]. A self-standing and flexible membrane based on $CaCO_3$/Teflon with ionic conductivity of 2.4 mS cm^{-1} was employed as a separator for a graphite anode and Li-containing cathodes [53]. The size of the ceramic particles showed great influence on characteristics as well as electrochemical performance. For instance, Al_2O_3 separator with the smaller size (0.01 μm) showed higher electrolyte affinity than Al_2O_3 separator with a larger size (0.3 μm), resulting in improved cycling performance. The thermal analysis indicated that the separators with smaller-size particles exhibited less thermal shrinkage, as the smaller particles required less binder content to fabricate separators. In contrast, the separators with large-size particles resulted in high thermal shrinkage due to the decomposition of polymeric binders, as larger particle size required high binder content to fabricate separators [54]. The graphite/$LiFePO_4$ cell comprising an Al_2O_3 membrane showed higher coulombic efficiency (77.9%) than the cell comprising Celgard 2400 separator (75.6%), which is attributed to the capturing of a trace amount of water and acidic impurity in the electrolyte by the Al_2O_3 membrane [242]. The graphite/$LiFePO_4$ full cell comprising Al_2O_3 and SiO_2 membranes displayed acceptable capacity retention (~60%) even at the low temperature of −20 °C [243]. The Al_2O_3 separator was prepared by coating an Al_2O_3 layer on commercial paper through spray coating technology. The resulting separator manifested stable cycling performance for the graphite/$LiCoO_2$ full cell with capacity retention of 90% after 65 cycles in 1 M $LiPF_6$ in EC/DMC electrolyte [244]. Glass fiber mat was fabricated through a wet-laid process using porous PVDF binder, and the resulting separator exhibited good cycling performance for the graphite/NMC cathode [245]. The Li/$LiCoO_2$ cathode comprising TiO_2 nanoparticles dispersed glass fiber displayed outstanding cycling performance with a capacity retention of 80% after 1500 cycles [246]. The pure Al_2O_3 nanowires-based membrane was fabricated through a filtration approach without using binder, and the resulting separator immersed in Li/$LiFePO_4$ cell exhibited stable cycling performance at 120 °C [247]. Ceramic membrane separators such as Al_2O_3 and zeolitic imidazolite framework (ZIF) were directly coated onto the electrode materials, and the resulting electrode exhibited stable electrochemical performance [248,249]. Although ceramic-based separators show acceptable performance, their poor mechanical property and low ionic conductivity are major drawbacks. The characteristics and electrochemical performance of the ceramic composite separators are listed in Table 8.

5.4. Nature-inspired separators

Considering the environmental impact and cost of synthetic polymers, naturally occurring polymers were employed as separators because of their low cost and environmental friendliness. Various natural cellulose derivatives such as cladophora cellulose [250] and commercial rice paper [251] were employed as separators for LIBs. These membranes exhibited porosity of 46%, electrolyte uptake of 250% due to the existence of hydrophilic OH and COOH groups, and thermal stability up to 150 °C. The graphite anodes and $LiFePO_4$, $LiCoO_2$, and $LiMn_2O_4$ cathodes comprising these membranes demonstrated good rate performance and cycling performance, which are comparable to the cells comprising commercial separator [251]. Lignin, an organic polymer fiber, showed ionic conductivity of 3.73 mS cm^{-1}, electrolyte uptake of 230%, and an outstanding electrochemical stability window up to 7.5 V in 1 M $LiPF_6$ in EC/EMC/DMC electrolyte. Due to these intriguing properties, lignin gel polymer electrolyte exhibited excellent compatibility with both anodes and cathodes [252]. Prawn shell-derived chitin nanofiber membrane exhibited stable voltage profile for a Li/$LiFePO_4$ cell in 1 M $LiPF_6$ in EC/DEC electrolyte, even at 120 °C [253]. Silk fibroin membranes demonstrated high porosity (60%) and large electrolyte affinity (1111%), and the Li/$LiFePO_4$ cathode cell comprising silk fibroin membrane showed stable cycling performance with the capacity retention of 99.5% for 50 cycles [254]. Sisal fiber-based separators were produced through a papermaking process, and the resulting separators exhibited high electrolyte affinity and a large electrochemical stability window up to 5.2 V [255]. Although natural polymeric separators showed intriguing characteristics, the large pore size, low ionic conductivity, and weak mechanical properties

Table 8
The characteristics and electrochemical performance of ceramic-based membranes.

Separator material	Thickness (μm)	Porosity (%)	Ionic conductivity (mS cm ^{1})	Electrolyte uptake (%)	Mechanical strength (MPa)	Shrinkage Rate at Temp °C	Cell	Electrolyte	Capacity retention %	Ref
Al_2O_3 supported paper substrate	48	56	1.64	–	5.3	Nil at 130 °C	Graphite/ $LiCoO_2$	1 M $LiPF_6$/ EC/DMC	99% after 60 cycles	[244]
Glass fiber/PVDF/ TiO_2	65	58	3.45	330	–	Nil at 150 °C	Li/$LiCoO_2$	1 M $LiPF_6$/ EC/DMC/ EMC	80% after 1500 cycles	[246]
Glass fiber/PI	46	49	0.38	210	10.4	Nil at 200 °C	Li/$LiFePO_4$	1 M $LiPF_6$/ EC/DEC	86% after 50 cycles	[59]
Hydroxyapatite/ cellulose fibers	56	81	3.07	253	13.2	Nil at 200 °C	Li/$LiFePO_4$	1 M $LiPF_6$/ EC/DMC	97% after 150 cycles	[60]

are major limitations.

5.5. Redox-active separators

Redox-active functional materials have gained significant interest in batteries owing to their additional redox reactions, contributing to the additional specific capacity [256]. The redox-active groups were tethered on active electrode materials [257], electrolytes [258], polymeric binders [259], and separator membrane [260]. Redox-active polypyrrole was coated on the cellulose separator through a papermaking process, and the resulting separator showed high thermal stability with zero thermal shrinkage at 200 °C. The Li/$LiFePO_4$ cell polypyrrole/cellulose separator manifested the higher specific capacity (276 mAh g ^{1} at 0.2C) than that of commercial PE (152 mAh g ^{1}) due to the additional capacity contributed by the oxidation and reduction of polypyrrole [PPy + PF_6 ⇌ (PPy^{+}) PF_6 +e] [261]. The redox-active PDA functionalized cellulose membrane showed high ionic conductivity of 1.06 mS cm ^{1} and thermal stability up to 150 °C. The Li/$Li_4Ti_5O_{12}$ cell comprising PDA/CNT/cellulose separator manifested higher specific capacity (110 mAh g ^{1} at 5C) than the PE-based cell (70 mAh g ^{1} at 5C) [262]. Despite the enhancement in specific capacity, the incorporation of bulky redox-active groups increases the overall weight of the cell, which in turn reduces the energy density of the cell, inhibiting their potential for real applications. More importantly, the investigation of the chemical stability of redox-functional groups against the electrolyte and electrode components under oxidative/reduction conditions is of great importance.

5.6. Shutdown functionalized separators

Shutdown functionality is an important feature for developing safe LIBs. The state-of-the-art PP/PE/PP multilayer separators shows shutdown function in the temperature range between 130 °C and 165 °C. However, after the pore closure of PE at 130 °C, the temperature of the cell may still increase, causing the melting of the PP layers and the shrinkage of the whole separator, leading to internal shorting. In some cases, the increase in temperature may lead to catastrophic thermal failure. Due to the critical buffer temperature (35 °C), preventing catastrophic battery failure is a tedious task. Various shutdown functional separators with wide buffer temperature were reported. For instance, the PBI/PE sandwiched structure showed shutdown function at 140 °C due to the melting of the inner PE layer, while the outer PBI layer remained porous and maintained dimensional stability up to 200 °C [96]. The PE/PI and PE/PET separators showed shutdown function at 130 °C and remained stable up to 200 °C [263,264]. Multi-layer separator comprising PE/Al_2O_3/PP and boehmite/PE displayed shutdown function at 130 °C, ensuring promising shutdown functionality [265,266]. A core/shell PAN/poly(butylene succinate) exhibited shutdown function at 110 °C due to the melting of the PBS layer, while the PAN layer preserved the thermal integrity of the membrane up to 250 °C [267]. The poly(butylene succinate) functionalized polylactide membrane demonstrated prompt shutdown function at 130 °C and preserved the dimensional stability of the membrane up to 170 °C due to the thermal stability of the polylactide backbone [268]. The PVDF/PET hybrid membrane exhibited shutdown function at 130 °C and maintained the physical dimensional stability until 250 °C due to the presence of a thermally stable PET backbone [198]. Some of the nonwoven-based shutdown functionalized membranes such as PAN/-polyurethane [269], PVDF/poly (*m*-phenyleneisothalamide) [270], and PEEK/PMMA [271] demonstrated shutdown temperature over 170 °C. The characteristics and shutdown functionality of various separator membranes are listed in Table 9.

6. Overall trend of separator membranes

The substantial research efforts on separator membranes have led to the development of wide arrays of separator membranes such as functionalized polyolefin separators, polyolefin/nonwoven multilayer separators, nonwoven separators, and ceramic composite separators. The polymer and ceramic functionalized polyolefin separators showed electrolyte affinity up to 250% and thermal stability at 150–170 °C. The nonwoven membrane displayed large electrolyte uptake up to 500% and high thermal stability up to 250 °C. The polymer and ceramic functionalized nonwoven membrane exhibited shutdown function at 130 °C and high ionic conductivity up to 5 mScm ^{1}. Nevertheless, the polymer and ceramic functionalization showed negligible effect on pore size and porosity reduction. Ceramic composite separators exhibited good electrolyte affinity (150%) and better thermal properties (~150 °C); however, weak mechanical strength and large pore size are the major limitations. The multilayer separators based on polyolefin and nonwoven membranes showed prompt shutdown function at 130 °C, maintained separator integrity until 200 °C, and demonstrated larger buffer temperature (70 °C), indicating their great potential as separators for future applications. The categorization of evolution of different types of separator membrane and overall advantages and disadvantages of the separator membranes are shown in Fig. 5.

7. Conclusions and future perspectives

A separator is located between the positive and negative electrodes in a LIB cell to physically isolate the two electrodes while permitting ionic conduction via the electrolyte. The characteristics of separators, such as thickness, porosity, pore size, electrolyte affinity, mechanical strength, and melting point, influence the charge/discharge behavior, rate performance, cycle stability, reliability and safety of LIBs. Single-layer and trilayer polyolefin microporous separators have been employed in commercial LIBs. Polyolefin separators are characterized with various thickness ranging from 18 to 25 μm, high porosity (40%), pore size (50–100 Å), and mechanical strength of 120 MPa. Nevertheless, the low electrolyte affinity (<100%) and thermal shrinkage even at low temperature (120 °C for PE and 150 °C for PP) affect the efficiency as well as safety of LIBs. Various approaches have been employed to

Table 9
The characteristics, electrochemical performance, and shutdown functionality of various separator. membranes.

Separator material	Thickness (μm)	Porosity (%)	Ionic conductivity (mS cm ^{1})	Electrolyte uptake (%)	Mechanical strength (MPa)	Shutdown Temp (°C)	Cell	Capacity retention	Ref
PE/PBI	28	54	0.59	225	NA	140–200	Li/$LiFePO_4$	97.7% after 100 cycles	[96]
PE/PI	26	60	1.34	400	NA	120–200	Li/$LiMn_2O_4$	96.4% after 100 cycles	[263]
PE/PET	22	65	0.58	60	NA	140–200	Graphite/ $LiCoO_2$	97.1% after 90 cycles	[264]
PAN/PBS	NA	59.3	2.1	665	NA	110–250	Li/$LiFePO_4$	93.2% after 100 cycles	[267]
PVDF/PMIA	45	72.9	1.7	753	NA	180	Li/$LiCoO_2$	93.6% after 100 cycles	[270]
PEEK/PMMA	12.7	64.1	NA	172.8	NA	270	Li/LMNCO	NA	[271]

Fig. 5. Categorization of the evolution of separators and the overall advantages and disadvantages of various types of separators.

mitigate the challenges associated with polyolefin separators. Of them, radiation techniques such as electron beam irradiation, oxygen plasma, and gamma radiation techniques have been employed to tune the surface characteristics of the rigid polyolefin separators. While these treatments can improve the electrolyte affinity, the high-energy radiation can penetrate several nanometers deep from the surface of the pristine membrane, which can reduce the tensile and puncture strength of the polyolefin separators. Controlling the radiation dose and reaction time is critical to achieving reasonable electrolyte affinity without affecting the inherent porosity of the separator membrane. Furthermore, although radiation approach has been used to improve the electrolyte affinity, it showed a negligible effect on the thermal stability of the polyolefin membrane.

Functionalization of polyolefin separators using organic molecules or polymeric materials can improve the electrolyte affinity as well as thermal properties. The functionalization using a porous polymer skeleton such as PVDF and PEI led to the thin porous coating, preserving the porous structure of the pristine separator membrane. In contrast, functionalization using high molecular weight polymers such as PMMA, PI, and PET resulted in a dense coating layer, which blocks the pores and increases the overall thickness of the separator, affecting the ionic transport kinetics of the cell. Achieving a coating thickness (up to few nanometers) is critical to preserve the porous structure of the base separator. Polyelectrolyte is one of the most important coating materials, which led to formation of thin coating (less than 10 nm) and improved the electrolyte affinity without affecting the inherent characteristics of polyolefin separators.

Incorporation of ceramic layers onto the base separator is another effective approach, resulting in significant improvement in electrolyte wetting and thermal dimensional stability. Characteristics of ceramic materials play a dominant role in dictating the properties of the ceramic functionalized polyolefin separator. The ceramic layer comprising zero-dimensional nanoparticles can be homogenously distributed over the base separator, resulting in partial blockage of pores and preserving the intrinsic characteristics of the base separator. In contrast, the deposition of one-dimensional nanowires/nanorods and three-dimensional spheres resulted in random distribution and led to severe blockage of pores. Besides, the size of the ceramic particles influences the characteristics of the separator. Nanoparticles with the size in the range of 20 nm–100 nm can be distributed homogeneously, while the larger particles resulted in random distribution and blocked the pores.

Numerous approaches have been employed to facilitate polymer and ceramic functionalization on the base separators. A solution phase dip-coating strategy has been widely employed to deposit various polymers and ceramic materials. The dip-coating approach led to the formation of polymer or ceramic coating on both sides of the separators. Although coating on both sides of separators can enhance the thermal stability and improve tensile strength; however, it can lead to significant pore blockage, affecting the function of the separators. The polymer-based dip-coating approach can be involved without using additives, whereas ceramic functionalization required polymeric binder, which helps to produce a homogenous ceramic coating slurry and improves the adhesion strength between the ceramic layer and base separator. The polymeric binder with a high melting point is critical to maintain the thermal stability of ceramic modified polyolefin separators. Although dip-coating approach has been widely employed, controlling the thickness of the functional materials is a challenging task. Layer-by-layer assembly and self-assembly are the alternate approaches, both of which can yield specific control over the thickness of the functional coating materials. A dry approach such as ALD is an effective approach to deposit ceramic materials due to its control over thickness. The ALD technique can provide a thin coating (~6 nm), which preserves the porosity and pores of the base separator. Overall, the modification of polyolefin separators with polymeric and ceramic materials improved electrolyte affinity, thermal stability, and ionic conductivity.

Nonwoven-based separators exhibited open porous structure with the porosity around 80%, ionic conductivity up to 5 mS cm ^{1}, and high electrolyte affinity up to 500%. Despite these merits, the large pore size (over 2 μm) and high porosity (above 80%) are the major limitations. The high porosity can reduce the tensile and puncture strength and the large pore size allows physical contact between the negative and positive electrodes, causing internal short circuit and cell failure. Further, nonwoven membrane cannot shut down the battery promptly due to high melt integrity (over 200 °C), posing a severe safety risk. Modification of nonwoven separators using polymer matrices is a promising approach, resulting in porosity below 50% and pore size less than 1 μm. In addition, functionalization of nonwoven membrane using polymers with low melt integrity (150 °C) such as PVDF promptly shut down the battery within the safe temperature limit (~130 °C). The ceramic deposition on the nonwoven membrane occurred at the surface of the fibrous structure, showing negligible influence on reduction of porosity and pore size. The ceramic functionalized nonwoven separators showed high electrolyte affinity and shutdown functionality. However, diminishing the large porosity and pore size is crucial to prevent internal shorting and ensure safety of a cell.

Ceramic separators showed high ionic conductivity, high porosity, and high thermal stability. Despite these merits, the large thickness (up to 200 μm) and low mechanical properties (less than 20 MPa) impede their large-scale applications. Moreover, the ceramic separators showed significant thermal shrinkage over 20% even at 150 °C, which is attributed to the decomposition of polymeric binders. Choosing thermally stable binders is a key criterion to enhance thermal shrinkage of the ceramic separators. The nature-inspired polymers exhibited large porosity and high electrolyte affinity; however, the large thickness over 100 μm and poor mechanical strength are the major hurdles. Redox-active separators showed improvement in specific capacity due to the additional contribution through redox-reaction; however, the incorporation of redox-active groups onto the base separator is a tedious and time-consuming task, limiting their possible implementation for large-scale applications. More importantly, the investigation of chemical stability of the redox-active groups against the electrolyte under oxidative/reductive conditions in a different temperature range (from 0 °C to 60 °C) is critically required. Any possible dissolution of redox-active groups can block the porous structure of the membrane and thereby diminishes the ionic transport between the electrodes.

Overall, recent advances in separator technology have shown substantial advances in both polyolefin and non-polyolefin separators. Nevertheless, most of these advancements are still in the laboratory scale. Ceramic modified polyolefin separators are under large-scale production to target electric vehicle applications. Nonwoven-based separators also provide an opportunity for mass production. Nonwoven membranes such as PI and PET considered promising due to their high structural stability, low-cost, high thermal stability, presenting great potential as separators for commercial applications. Evonik Industry has manufactured the ceramic functionalized PET membrane (Separion P20) for large-scale consumer electronics applications. Further, research advances on separator membrane technology are performed mainly at room temperature and occasionally at elevated temperature (up to 120 °C); however, investigation of the separator membrane at a lower temperature has been rarely carried out. The electrochemical investigation of separator membranes at low temperature (from 0 to 20 °C) may provide guidance for developing batteries to be used in cold geographical regions. The Al_2O_3 based ceramic composite separators can work efficiently at low temperature (20 °C), showing great potential as separator in LIBs for low-temperature applications.

One of the concerns with the current separator technology is that advancements are limited to graphite anode and lithium-based cathodes, which are approaching the specific capacity limits. The development of separator membranes for most promising electrode materials for future battery technology such as high-capacity cathodes (NMC, NCA, and sulfur) and high-capacity anodes such as silicon, germanium, and

tin is of paramount importance.

Credit author statement

Niranjanmurthi Lingappan: Conceptualization, Design, Data curation, Visualization, Supervision, Project administration, Writing – original draft, and Review and Editing. Wonoh Lee: Review and Editing. Stefano Passerini: Writing, Review, and Editing. Michael Pecht: Conceptualization, Supervision, Project administration, Writing, Review, and Editing.

Declaration of competing interest

The authors declare that they have no known competing financial interests or personal relationships that could have appeared to influence the work reported in this paper.

Data availability

No data was used for the research described in the article.

Acknowledgement

The authors thank the more than 150 companies and organizations that support research activities at the Center for Advanced Life Cycle Engineering (CALCE) at the University of Maryland, United States and the Centre for Advanced Innovations in Reliability and Safety (CAIRS) in conjunction with Polytechnic University of Hong Kong. S.P. acknowledges the basic funding from the Helmholtz Association, Germany. N.L. acknowledges the research support from the National Research Foundation of Korea, South Korea (NRF) under the R&D project No: RS-2023-00248047.

References

[1] Jaiswal A. Lithium-ion battery based renewable energy solution for off-grid electricity: a techno-economic analysis. Renew. Sust. Energy Rev. 2017;72: 922–34.
[2] Wang Q, Sun J, Chu G. Lithium ion battery fire and explosion. Fire Saf Sci 2005;8: 375–82.
[3] Williard N, He W, Hendricks C, Pecht M. Lessons learned from the 787 dreamliner issue on lithium-ion battery reliability. Energies 2013;6:4682–95.
[4] Huang X. Separator technologies for lithium-ion batteries. J Solid State Electrochem 2011;15:649–62.
[5] Orendorff CJ. The role of separators in lithium-ion cell safety. Interface 2012;21: 61–5.
[6] Yoneda H, Nishimura Y, Doi Y, Fukuda M, Kohno M. Development of microporous PE films to improve lithium ion batteries. Polym J 2010;42:425–37.
[7] Wang Q, Ping P, Zhao X, Chu G, Sun J, Chen C. Thermal runaway caused fire and explosion of lithium ion battery. J Power Sources 2012;208:210–24.
[8] Liu B, Jia Y, Yuan C, Wang L, Gao X, Yin S, Xu J. Safety issues and mechanisms of lithium-ion battery cell upon mechanical abusive loading: a review. Energy Storage Mater 2020;24:85–112.
[9] Xu B, Lee J, Kwon D, Kong L, Pecht M. Mitigation strategies for Li-ion battery thermal runaway: a review. Renew. Sust. Energy Rev. 2021;150:111437.
[10] Arora P, Zhang Z. Battery separators. Chem Rev 2004;104:4419–62.
[11] Zhang SS. A review on the separators of liquid electrolyte Li-ion batteries. J Power Sources 2007;164:351–64.
[12] Waqas M, Ali S, Feng C, Chen D, Han J, He W. Recent development in separators for high-temperature lithium-ion batteries. Small 2019;15:1901689.
[13] Lee H, Yanilmaz M, Toprakci O, Fu K, Zhang X. A review of recent developments in membrane separators for rechargeable lithium-ion batteries. EnergyEnviron. Sci. 2014;7:3857–86.
[14] Lagadec MF, Zahn R, Wood V. Characterization and performance evaluation of lithium-ion battery separators. Nat Energy 2019;4:16–25.
[15] Kritzer P. Nonwoven support material for improved separators in Li–polymer batteries. J Power Sources 2006;161:1335–40.
[16] Wang Y, Zhu S, Sun D, Jin Y. Preparation and evaluation of a separator with an asymmetric structure for lithium-ion batteries. RSC Adv 2016;6:105461–8.
[17] Hwang K, Kwon B, Byun H. Preparation of PVdF nanofiber membranes by electrospinning and their use as secondary battery separators. J Membr Sci 2011; 378:111–6.
[18] García-Gabaldón M, Pérez-Herranz V, Sánchez E, Mestre S. Effect of porosity on the effective electrical conductivity of different ceramic membranes used as separators in eletrochemical reactors. J Membr Sci 2006;280:536–44.
[19] Bladwin RS. A review of state-of-the-art separator materials for advanced lithium-based batteries for future aerospace Missions. 2009.
[20] Zhang F, Ma X, Cao C, Li J, Zhu Y. Poly(vinylidene fluoride)/SiO_2 composite membranes prepared by electrospinning and their excellent properties for nonwoven separators for lithium-ion batteries. J Power Sources 2014;251: 423–31.
[21] Venugopal G, Moore J, Howard J, Pendalwar S. Characterization of microporous separators for lithium-ion batteries. J Power Sources 1999;77:34–41.
[22] Ihm D, Noh J, Kim J. Effect of polymer blending and drawing conditions on properties of polyethylene separator prepared for Li-ion secondary battery. J Power Sources 2002;109:388–93.
[23] Djian D, Alloin F, Martinet S, Lignier H, Sanchez JY. Lithium-ion batteries with high charge rate capacity: influence of the porous separator. J Power Sources 2007;172:416–21.
[24] Lee Y, Park J, Jeon H, Yeon D, Kim BH, Cho KY, Ryou MY, Lee YM. In-depth correlation of separator pore structure and electrochemical performance in lithium-ion batteries. J Power Sources 2016;325:732–8.
[25] Xiang Y, Li J, Lei J, Liu D, Xie Z, Qu D, Li K, Deng T, Tang H. Advanced separators for lithium-ion and lithium–sulfur batteries: a review of recent progress. ChemSusChem 2016;9:3023–39.
[26] Zhang X, Sahraei E, Wang K. Li-Ion battery separators, mechanical integrity and failure mechanisms leading to soft and hard internal shorts. Sci Rep 2016;6: 32578.
[27] Kalnaus S, Wang Y, Turner JA. Mechanical behavior and failure mechanisms of Li-ion battery separators. J Power Sources 2017;348:255–63.
[28] Pfleging W, Pröll J. A new approach for rapid electrolyte wetting in tape cast electrodes for lithium-ion batteries. J Mater Chem A 2014;2:14918–26.
[29] Miao YE, Zhu GN, Hou H, Xia YY, Liu T. Electrospun polyimide nanofiber-based nonwoven separators for lithium-ion batteries. J Power Sources 2013;226:82–6.
[30] Cannarella J, Arnold CB. Ion transport restriction in mechanically strained separator membranes. J Power Sources 2013;226:149–55.
[31] Holtmann J, Schäfer M, Niemöller A, Winter M, Lex-Balducci A, Obeidi S. Boehmite-based ceramic separator for lithium-ion batteries. J Appl Electrochem 2016;46:69–76.
[32] Roth EP, Doughty DH, Pile DL. Effects of separator breakdown on abuse response of 18650 Li-ion cells. J Power Sources 2007;174:579–83.
[33] Patry G, Romagny A, Martinet S, Froelich D. Cost modeling of lithium-ion battery cells for automotive applications. Energy Sci Eng 2015;3:71–82.
[34] Huang X. Development and characterization of a bilayer separator for lithium ion batteries. J Power Sources 2011;196:8125–58.
[35] Zhang X, Sahraei E, Wang K. Deformation and failure characteristics of four types of lithium-ion battery separators. J Power Sources 2016;327:693–701.
[36] Xiong B, Chen R, Zeng F, Kang J, Men Y. Thermal shrinkage and microscopic shutdown mechanism of polypropylene separator for lithium-ion battery: in-situ ultra-small angle X-ray scattering study. J Membr Sci 2018;545:213–20.
[37] Deimede V, Elmasides C. Separators for lithium-ion batteries: a review on the production processes and recent developments. Energy Technol 2015;3:453–68.
[38] Zhang X, Ji L, Toprakci O, Liang Y, Alcoutlabi M. Electrospun nanofiber-based anodes, cathodes, and separators for advanced lithium-ion batteries. Polym Rev 2011;51:239–64.
[39] Zhang J, Liu Z, Kong Q, Zhang C, Pang S, Yue L, Wang X, Yao J, Cui G. Renewable and superior thermal-resistant cellulose-based composite nonwoven as lithium-ion battery separator. ACS Appl Mater Interfaces 2013;5:128–34.
[40] Yuan B, He N, Liang Y, Dong L, Liu J, Han J, He W, Liu Y. A surfactant-modified composite separator for high safe lithium ion battery. J Energy Chem 2023;76: 398–403.
[41] Liang Y, Cheng S, Zhao J, Zhang C, Sun S, Zhou N, Qiu Y, Zhang X. Heat treatment of electrospun Polyvinylidene fluoride fibrous membrane separators for rechargeable lithium-ion batteries. J Power Sources 2013;240:204–11.
[42] Xiao W, Zhao L, Gong Y, Liu J, Yan C. Preparation and performance of poly(vinyl alcohol) porous separator for lithium-ion batteries. J Membr Sci 2015;487:221–8.
[43] Cho TH, Tanaka M, Onishi H, Kondo Y, Nakamura T, Yamazaki H, Tanase S, Sakai T. Battery performances and thermal stability of polyacrylonitrile nanofiber-based nonwoven separators for Li-ion battery. J Power Sources 2008;181: 155–60.
[44] Hao J, Lei G, Li Z, Wu L, Xiao Q, Wang L. A novel polyethylene terephthalate nonwoven separator based on electrospinning technique for lithium ion battery. J Membr Sci 2013;428:11–6.
[45] Kong L, Liu B, Ding J, Yan X, Tian G, Qi S, Wu D. Robust polyetherimide fibrous membrane with crosslinked topographies fabricated via in-situ micro-melting and its application as superior Lithium-ion battery separator with shutdown function. J Membr Sci 2018;549:244–50.
[46] Yanilmaz M, Dirican M, Zhang X. Evaluation of electrospun SiO_2/nylon 6,6 nanofiber membranes as a thermally-stable separator for lithium-ion batteries. Electrochim Acta 2014;133:501–8.
[47] Huang X. A lithium-ion battery separator prepared using a phase inversion process. J Power Sources 2012;216:216–21.
[48] Li D, Shi D, Feng K, Li X, Zhang H. Poly (ether ether ketone) (PEEK) porous membranes with super high thermal stability and high rate capability for lithium-ion batteries. J Membr Sci 2017;530:125–31.
[49] Li D, Shi D, Xia Y, Qiao L, Li X, Zhang H. Superior thermally stable and nonflammable porous polybenzimidazole membrane with high wettability for high-power lithium-ion batteries. ACS Appl Mater Interfaces 2017;9:8742–50.
[50] Zhang H, Zhang Y, Xu T, John AE, Li Y, Li W, Zhu B. Poly(m-phenylene isophthalamide) separator for improving the heat resistance and power density of lithium-ion batteries. J Power Sources 2016;329:8–16.

[51] Liu J, Qin J, Mo Y, Wang S, Han D, Xiao M, Meng Y. Polyphenylene sulfide separator for high safety lithium-ion batteries. J Electrochem Soc 2019;166: A1644–52.
[52] Gugliuzza A, Drioli E. A review on membrane engineering for innovation in wearable fabrics and protective textiles. J Membr Sci 2013;446:350–75.
[53] Zhang SS, Xu K, Jow TR. An inorganic composite membrane as the separator of Li-ion batteries. J Power Sources 2005;140:361–4.
[54] Takemura D, Aihara S, Hamano K, Kise M, Nishimura T, Urushibata H, Yoshiyasu H. A powder particle size effect on ceramic powder based separator for lithium rechargeable battery. J Power Sources 2005;146:779–83.
[55] Chen J, Wang S, Cai D, Wang H. Porous SiO_2 as a separator to improve the electrochemical performance of spinel $LiMn_2O_4$ cathode. J Membr Sci 2014;449: 169–75.
[56] Raja M, Sanjeev G, Prem Kumar T, Manuel Stephan A. Lithium aluminate-based ceramic membranes as separators for lithium-ion batteries. Ceram Int 2015;41: 3045–50.
[57] Raja M, Sanjeev G, Prem Kumar T, Manuel Stephan A. Lithium aluminate-based ceramic membranes as separators for lithium-ion batteries. Ceram Int 2015;41: 3045–50.
[58] Suriyakumar S, Raja M, Angulakshmi N, Nahm KS, Stephan AM. A flexible zirconium oxide based-ceramic membrane as a separator for lithium-ion batteries. RSC Adv 2016;6:92020–7.
[59] Zhang B, Wang Q, Zhang J, Ding G, Xu G, Liu Z, Cui G. A superior thermostable and nonflammable composite membrane towards high power battery separator. Nano Energy 2014;10:277–87.
[60] Li H, Wu D, Wu J, Dong LY, Zhu YJ, Hu X. Flexible, high-wettability and fire-resistant separators based on hydroxyapatite nanowires for advanced lithium-ion batteries. Adv Math 2017;29:1703548.
[61] Jung YC, Kim SK, Kim MS, Lee JH, Han MS, Kim DH, Shin WC, Ue M, Kim DW. Ceramic separators based on Li^+-conducting inorganic electrolyte for high-performance lithium-ion batteries with enhanced safety. J Power Sources 2015; 293:675–83.
[62] Shin WK, Kim DW. High performance ceramic-coated separators prepared with lithium ion-containing SiO_2 particles for lithium-ion batteries. J Power Sources 2013;226:54–60.
[63] Wang W, Li Y, Cheng L, Zuo F, Yang S. Safety performance and failure prediction model of cylindrical lithium-ion battery. J Power Sources 2020;451:227755.
[64] Lingappan N, Kong L, Pecht M. The significance of aqueous binders in lithium-ion batteries. Renew. Sust. Energy Rev. 2021;147:111227.
[65] Ren F, Cox T, Wang H. Thermal runaway risk evaluation of Li-ion cells using a pinch–torsion test. J Power Sources 2014;249:156–62.
[66] Sarkar A, Shrotriya P, Chandra A. Modeling of separator failure in lithium-ion pouch cells under compression. J Power Sources 2019;435:226756.
[67] Zhang ZJ, Ramadass P. Lithium-ion battery separators. In: Yoshio M, Brodd RJ, Kozawa A, editors. Lithium-ion batteries: Science and Technologies. New York, NY: Springer New York; 2009. p. 1–46.
[68] Sheidaei A, Xiao X, Huang X, Hitt J. Mechanical behavior of a battery separator in electrolyte solutions. J Power Sources 2011;196:8728–34.
[69] Xie W, Liu W, Dang Y, Tang A, Deng T, Qiu W. Investigation on electrolyte-immersed properties of lithium-ion battery cellulose separator through multi-scale method. J Power Sources 2019;417:150–8.
[70] Yan S, Xiao X, Huang X, Li X, Qi Y. Unveiling the environment-dependent mechanical properties of porous polypropylene separators. Polym 2014;55: 6282–92.
[71] Gor GY, Cannarella J, Leng CZ, Vishnyakov A, Arnold CB. Swelling and softening of lithium-ion battery separators in electrolyte solvents. J Power Sources 2015; 294:167–72.
[72] Seong IW, Hong CH, Kim BK, Yoon WY. The effects of current density and amount of discharge on dendrite formation in the lithium powder anode electrode. J Power Sources 2008;178:769–73.
[73] Jana A, Ely DR, García RE. Dendrite-separator interactions in lithium-based batteries. J Power Sources 2015;275:912–21.
[74] Zhang SS, Fan X, Wang C. Preventing lithium dendrite-related electrical shorting in rechargeable batteries by coating separator with a Li-killing additive. J Mater Chem A 2018;6:10755–60.
[75] Barai P, Higa K, Srinivasan V. Lithium dendrite growth mechanisms in polymer electrolytes and prevention strategies. Phys Chem Chem Phys 2017;19: 20493–505.
[76] Mao B, Chen H, Cui Z, Wu T, Wang Q. Failure mechanism of the lithium ion battery during nail penetration. Int J Heat Mass Tran 2018;122:1103–15.
[77] Zubi G, Dufo-López R, Carvalho M, Pasaoglu G. The lithium-ion battery: state of the art and future perspectives. Renew. Sust. Energy Rev. 2018;89:292–308.
[78] Kostecki R, Norin L, Song X, McLarnon F. Diagnostic studies of polyolefin separators in high-power Li-ion cells. J Electrochem Soc 2004;151:A522.
[79] Shi J, Xia Y, Yuan Z, Hu H, Li X, Zhang H, Liu Z. Porous membrane with high curvature, three-dimensional heat-resistance skeleton: a new and practical separator candidate for high safety lithium ion battery. Sci Rep 2015;5:8255.
[80] Lai WJ, Ali MY, Pan J. Mechanical behavior of representative volume elements of lithium-ion battery cells under compressive loading conditions. J Power Sources 2014;245:609–23.
[81] Sahraei E, Hill R, Wierzbicki T. Calibration and finite element simulation of pouch lithium-ion batteries for mechanical integrity. J Power Sources 2012;201: 307–21.
[82] Kim KJ, Kim YH, Song JH, Jo YN, Kim JS, Kim YJ. Effect of gamma ray irradiation on thermal and electrochemical properties of polyethylene separator for Li ion batteries. J Power Sources 2010;195:6075–80.
[83] Jiang Q, Li Z, Wang S, Zhang H. A separator modified by high efficiency oxygen plasma for lithium ion batteries with superior performance. RSC Adv 2015;5: 92995–3001.
[84] Jin SY, Manuel J, Zhao X, Park WH, Ahn JH. Surface-modified polyethylene separator via oxygen plasma treatment for lithium ion battery. J. Indus. Eng. Chem. 2017;45:15–21.
[85] Kim KJ, Park MS, Yim T, Yu JS, Kim YJ. Electron-beam-irradiated polyethylene membrane with improved electrochemical and thermal properties for lithium-ion batteries. J Appl Electrochem 2014;44:345–52.
[86] Park JH, Park W, Kim JH, Ryoo D, Kim HS, Jeong YU, Kim DW, Lee SY. Close-packed poly(methyl methacrylate) nanoparticle arrays-coated polyethylene separators for high-power lithium-ion polymer batteries. J Power Sources 2011; 196:7035–8.
[87] Ryou MH, Lee YM, Park JK, Choi JW. Mussel-inspired polydopamine-treated polyethylene separators for high-power Li-ion batteries. Adv Mater 2011;23: 3066–70.
[88] Xiong M, Tang H, Wang Y, Pan M. Ethylcellulose-coated polyolefin separators for lithium-ion batteries with improved safety performance. Carbohydr Polym 2014; 101:1140–6.
[89] Shi JL, Fang LF, Li H, Zhang H, Zhu BK, Zhu LP. Improved thermal and electrochemical performances of PMMA modified PE separator skeleton prepared via dopamine-initiated ATRP for lithium ion batteries. J Membr Sci 2013;437: 160–8.
[90] Man C, Jiang P, Wong KW, Zhao Y, Tang C, Fan M, Lau W, Mei J, Li S, Liu H, Hui D. Enhanced wetting properties of a polypropylene separator for a lithium-ion battery by hyperthermal hydrogen induced cross-linking of poly(ethylene oxide). J Mater Chem A 2014;2:11980–6.
[91] Li B, Li Y, Dai D, Chang K, Tang H, Chang Z, Wang C, Yuan X, Wang H. Facile and nonradiation pretreated membrane as a high conductive separator for Li-ion batteries. ACS Appl Mater Interfaces 2015;7:20184–9.
[92] Gong S, Jeon H, Lee H, Ryou MH, Lee YM. Effects of an integrated separator/electrode assembly on enhanced thermal stability and rate capability of lithium-ion batteries. ACS Appl Mater Interfaces 2017;9:17814–21.
[93] Yue L, Zhang J, Liu Z, Kong Q, Zhou X, Xu Q, Yao J, Cui G. A heat resistant and flame-retardant polysulfonamide/polypropylene composite nonwoven for high performance lithium ion battery separator. J Electrochem Soc 2014;161: A1032–8.
[94] Han M, Kim DW, Kim YC. Charged polymer-coated separators by atmospheric plasma-induced grafting for lithium-ion batteries. ACS Appl Mater Interfaces 2016;8:26073–81.
[95] Yu J, Dong N, Liu B, Tian G, Qi S, Wu D. A newly-developed heat-resistance polyimide microsphere coating to enhance the thermal stability of commercial polyolefin separators for advanced lithium-ion battery. Chem Eng J 2022;442: 136314.
[96] Li D, Shi D, Yuan Z, Feng K, Zhang H, Li X. A low cost shutdown sandwich-like composite membrane with superior thermo-stability for lithium-ion battery. J Membr Sci 2017;542:1–7.
[97] Yoo Y, Kim BG, Pak K, Han SJ, Song HS, Choi JW, Im SG. Initiated chemical vapor deposition (iCVD) of highly cross-linked polymer films for advanced lithium-ion battery separators. ACS Appl Mater Interfaces 2015;7:18849–55.
[98] Huang Z, Chen Y, Han Q, Su M, Liu Y, Wang S, Wang H. Vapor-induced phase inversion of poly (m-phenylene isophthalamide) modified polyethylene separator for high-performance lithium-ion batteries. Chem Eng J 2022;429:132429.
[99] Zhang X, Li N, Hu Z, Yu J, Wang Y, Zhu J. Poly(p-phenylene terephthalamide) modified PE separators for lithium ion batteries. J Membr Sci 2019;581:355–61.
[100] Gu QQ, Xue HJ, Li ZW, Song JC, Sun ZY. High-performance polyethylene separators for lithium-ion batteries modified by phenolic resin. J Power Sources 2021;483:229155.
[101] Qiangfeng XAM, Li Y, Zhongyi L, Mei C. Lithium-based battery separator and method for making the same. U.S. Pat. No. 10128481B2; 2018.
[102] Yu C. Aramid fiber coats heat-resisting lithium ion battery separator and preparation method thereof. CN. Pat. No. 109904368A; 2021.
[103] Rao MM, Liu JS, Li WS, Liang Y, Zhou DY. Preparation and performance analysis of PE-supported P(AN-co-MMA) gel polymer electrolyte for lithium ion battery application. J Membr Sci 2008;322:314–9.
[104] Zahn R, Lagadec MF, Hess M, Wood V. Improving ionic conductivity and lithium-ion transference number in lithium-ion battery separators. ACS Appl Mater Interfaces 2016;8:32637–42.
[105] Choi JA, Kim SH, Kim DW. Enhancement of thermal stability and cycling performance in lithium-ion cells through the use of ceramic-coated separators. J Power Sources 2010;195:6192–6.
[106] Jeong HS, Lee SY. Closely packed SiO_2 nanoparticles/poly(vinylidene fluoride-hexafluoropropylene) layers-coated polyethylene separators for lithium-ion batteries. J Power Sources 2011;196:6716–22.
[107] Xu Q, Yang J, Dai J, Yang Y, Chen X, Wang Y. Hydrophilization of porous polypropylene membranes by atomic layer deposition of TiO_2 for simultaneously improved permeability and selectivity. J Membr Sci 2013;448:215–22.
[108] Li J, Chen L, Wang F, Qin Z, Zhang Y, Zhang N, Liu X, Chen G. Anionic metal-organic framework modified separator boosting efficient Li-ion transport. Chem Eng J 2023;451:138536.
[109] Kim KJ, Kwon HK, Park MS, Yim T, Yu JS, Kim YJ. Ceramic composite separators coated with moisturized ZrO_2 nanoparticles for improving the electrochemical performance and thermal stability of lithium ion batteries. Phys Chem Chem Phys 2014;16:9337–43.

[110] Yang C, Tong H, Luo C, Yuan S, Chen G, Yang Y. Boehmite particle coating modified microporous polyethylene membrane: a promising separator for lithium ion batteries. J Power Sources 2017;348:80–6.
[111] Yeon D, Lee Y, Ryou MH, Lee YM. New flame-retardant composite separators based on metal hydroxides for lithium-ion batteries. Electrochim Acta 2015;157: 282–9.
[112] Jung B, Lee B, Jeong YC, Lee J, Yang SR, Kim H, Park M. Thermally stable non-aqueous ceramic-coated separators with enhanced nail penetration performance. J Power Sources 2019;427:271–82.
[113] Herle SP. Battery separator with dielectric coating. U.S. Pat. No. 10411238B2; 2019.
[114] Feng G, Li Z, Mi L, Zheng J, Feng X, Chen W. Polypropylene/hydrophobic-silica-aerogel-composite separator induced enhanced safety and low polarization for lithium-ion batteries. J Power Sources 2018;376:177–83.
[115] Shekarian E, Jafari Nasr MR, Mohammadi T, Bakhtiari O, Javanbakht M. Preparation of 4A zeolite coated polypropylene membrane for lithium-ion batteries separator. J Appl Polym Sci 2019;136:47841.
[116] Qiu Z, Yuan S, Wang Z, Shi L, Jo JH, Myung ST, Zhu J. Construction of silica-oxygen-borate hybrid networks on Al_2O_3-coated polyethylene separators realizing multifunction for high-performance lithium ion batteries. J Power Sources 2020; 472:228445.
[117] Shi C, Zhang P, Chen L, Yang P, Zhao J. Effect of a thin ceramic-coating layer on thermal and electrochemical properties of polyethylene separator for lithium-ion batteries. J Power Sources 2014;270:547–53.
[118] Zhang P, Chen L, Shi C, Yang P, Zhao J. Development and characterization of silica tube-coated separator for lithium ion batteries. J Power Sources 2015;284: 10–5.
[119] Kim YB, Tran-Phu T, Kim M, Jung DW, Yi GR, Park JH. Facilitated ion diffusion in multiscale porous particles: application in battery separators. ACS Appl Mater Interfaces 2015;7:4511–7.
[120] Zhu X, Jiang X, Ai X, Yang H, Cao Y. TiO_2 ceramic-grafted polyethylene separators for enhanced thermostability and electrochemical performance of lithium-ion batteries. J Membr Sci 2016;504:97–103.
[121] Xu J, Xiao X, Zeng S, Cai M, Verbrugge MW. Multifunctional lithium-ion-exchanged zeolite-coated separator for lithium-ion batteries. ACS Appl Energy Mater 2018;1:7237–43.
[122] Le B. Battery separator and its constructing method, and lithium-on battery. US. Pat. No. 9620759; 2017.
[123] Rao MM, Liu JS, Li WS, Liao YH, Liang Y, Zhao LZ. Polyethylene-supported poly (acrylonitrile-co-methyl methacrylate)/nano-Al_2O_3 microporous composite polymer electrolyte for lithium ion battery. J Solid State Electrochem 2009;14: 255.
[124] Na W, Koh KH, Lee AS, Cho S, Ok B, Hwang SW, Lee JH, Koo CM. Binder-less chemical grafting of SiO_2 nanoparticles onto polyethylene separators for lithium-ion batteries. J Membr Sci 2019;573:621–7.
[125] Rahman MM, Mateti S, Cai Q, Sultana I, Fan Y, Wang X, Hou C, Chen Y. High temperature and high rate lithium-ion batteries with boron nitride nanotubes coated polypropylene separators. Energy Storage Mater 2019;19:352–9.
[126] Yu L, Jin Y, Lin YS. Ceramic coated polypropylene separators for lithium-ion batteries with improved safety: effects of high melting point organic binder. RSC Adv 2016;6:40002–9.
[127] Jeong HS, Kim DW, Jeong YU, Lee SY. Effect of phase inversion on microporous structure development of Al_2O_3/poly(vinylidene fluoride-hexafluoropropylene)-based ceramic composite separators for lithium-ion batteries. J Power Sources 2010;195:6116–21.
[128] Shi C, Dai J, Shen X, Peng L, Li C, Wang X, Zhang P, Zhao J. A high-temperature stable ceramic-coated separator prepared with polyimide binder/Al_2O_3 particles for lithium-ion batteries. J Membr Sci 2016;517:91–9.
[129] Wang J, Hu Z, Yin X, Li Y, Huo H, Zhou J, Li L. Alumina/phenolphthalein polyetherketone ceramic composite polypropylene separator film for lithium ion power batteries. Electrochim Acta 2015;159:61–5.
[130] Chen W, Shi L, Zhou H, Zhu J, Wang Z, Mao X, Chi M, Sun L, Yuan S. Water-based organic–inorganic hybrid coating for a high-performance separator. ACS Sustainable Chem Eng 2016;4:3794–802.
[131] Dong X, Mi W, Yu L, Jin Y, Lin YS. Zeolite coated polypropylene separators with tunable surface properties for lithium-ion batteries. Microporous Mesoporous Mater 2016;226:406–14.
[132] Peng K, Wang B, Li Y, Ji C. Magnetron sputtering deposition of TiO_2 particles on polypropylene separators for lithium-ion batteries. RSC Adv 2015;5:81468–73.
[133] Lee JW, Soomro AM, Waqas M, Khalid MAU, Choi KH. A highly efficient surface modified separator fabricated with atmospheric atomic layer deposition for high temperature lithium ion batteries. Int J Energy Res 2020;44:7035–46.
[134] Wang CP, Si W, Sim YL, Dieter T, Trassl R, Herle SP, Daube C, Zhu J, Cushing J. Ultra-thin ceramic coating on separator for batteries. US. Pat. No. 11588209B2. 2018.
[135] Kim M, Park JH. Inorganic thin layer coated porous separator with high thermal stability for safety reinforced Li-ion battery. J Power Sources 2012;212:22–7.
[136] Chen H, Lin Q, Xu Q, Yang Y, Shao Z, Wang Y. Plasma activation and atomic layer deposition of TiO_2 on polypropylene membranes for improved performances of lithium-ion batteries. J Membr Sci 2014;458:217–24.
[137] Im H, Wittenberg NJ, Lindquist NC, Oh SH. Atomic layer deposition: a versatile technique for plasmonics and nanobiotechnology. J Mater Res 2012;27:663–71.
[138] Kim HY, Kwack WS, Park MS. Ultra-thin ceramic coating on separator for batteries. U.S. Pat. No. 20170373295A1; 2017.
[139] Chao CH, Hsieh CT, Ke WJ, Lee LW, Lin YF, Liu HW, Gu S, Fu CC, Juang RS, Mallick BC, Gandomi YA. Roll-to-roll atomic layer deposition of titania coating on polymeric separators for lithium ion batteries. J Power Sources 2021;482:228896.
[140] Jung YS, Cavanagh AS, Gedvilas L, Widjonarko NE, Scott ID, Lee SH, Kim GH, George SM, Dillon AC. Improved functionality of lithium-ion batteries enabled by atomic layer deposition on the porous microstructure of polymer separators and coating electrodes. Adv Energy Mater 2012;2:1022–7.
[141] Kang SM, Ryou MH, Choi JW, Lee H. Mussel-and diatom-inspired silica coating on separators yields improved power and safety in Li-ion batteries. Chem Mater 2012;24:3481–5.
[142] Shin WK, Yoo JH, Kim DW. Surface-modified separators prepared with conductive polymer and aluminum fluoride for lithium-ion batteries. J Power Sources 2015;279:737–44.
[143] Wang Z, Guo F, Chen C, Shi L, Yuan S, Sun L, Zhu J. Self-assembly of PEI/SiO_2 on polyethylene separators for Li-ion batteries with enhanced rate capability. ACS Appl Mater & Interfaces 2015;7:3314–22.
[144] Pi JK, Wu GP, Yang HC, Arges CG, Xu ZK. Separators with biomineralized zirconia coatings for enhanced thermo- and electro-performance of lithium-ion batteries. ACS Appl Mater Interfaces 2017;9:21971–8.
[145] Yang P, Zhang P, Shi C, Chen L, Dai J, Zhao J. The functional separator coated with core–shell structured silica–poly(methyl methacrylate) sub-microspheres for lithium-ion batteries. J Membr Sci 2015;474:148–55.
[146] Xu W, Wang Z, Shi L, Ma Y, Yuan S, Sun L, Zhao Y, Zhang M, Zhu J. Layer-by-Layer deposition of organic–inorganic hybrid multilayer on microporous polyethylene separator to enhance the electrochemical performance of lithium-ion battery. ACS Appl Mater Interfaces 2015;7:20678–86.
[147] Dai J, Shi C, Li C, Shen X, Peng L, Wu D, Sun D, Zhang P, Zhao J. A rational design of separator with substantially enhanced thermal features for lithium-ion batteries by the polydopamine–ceramic composite modification of polyolefin membranes. Energy Environ Sci 2016;9:3252–61.
[148] Li J, Cheng S, Wang Z, Yu M, Zhi Q, Zhang X, Yan S. Multi-layered composite functional separator for lithium-ion battery. U.S. Pat. No. 2022;11(411):281.
[149] Zhu YS, Xiao SY, Li MX, Chang Z, Wang FX, Gao J, Wu YP. Natural macromolecule based carboxymethyl cellulose as a gel polymer electrolyte with adjustable porosity for lithium ion batteries. J Power Sources 2015;288:368–75.
[150] Li MX, Wang XW, Yang YQ, Chang Z, Wu YP, Holze R. A dense cellulose-based membrane as a renewable host for gel polymer electrolyte of lithium ion batteries. J Membr Sci 2015;476:112–8.
[151] Jiang F, Yin L, Yu Q, Zhong C, Zhang J. Bacterial cellulose nanofibrous membrane as thermal stable separator for lithium-ion batteries. J Power Sources 2015;279: 21–7.
[152] Kim H, Guccini V, Lu H, Salazar-Alvarez G, Lindbergh G, Cornell A. Lithium ion battery separators based on carboxylated cellulose nanofibers from Wood. ACS Appl Energy Mater 2019;2:1241–50.
[153] Cheng C, Yang R, Wang Y, Fu D, Sheng J, Guo X. A bacterial cellulose-based separator with tunable pore size for lithium-ion batteries. Carbohydr Polym 2023; 304:120489.
[154] Huang F, Xu Y, Peng B, Su Y, Jiang F, Hsieh YL, Wei Q. Coaxial electrospun cellulose-core fluoropolymer-shell fibrous membrane from recycled cigarette filter as separator for high performance lithium-ion battery. ACS Sustainable Chem Eng 2015;3:932–40.
[155] Xu Q, Kong Q, Liu Z, Wang X, Liu R, Zhang J, Yue L, Duan Y, Cui G. Cellulose/polysulfonamide composite membrane as a high performance lithium-ion battery separator. ACS Sustainable Chem Eng 2014;2:194–9.
[156] Xu Q, Kong Q, Liu Z, Zhang J, Wang X, Liu R, Yue L, Cui G. Polydopamine-coated cellulose microfibrillated membrane as high performance lithium-ion battery separator. RSC Adv 2014;4:7845–50.
[157] Guo T, Song J, Jin Y, Sun Z, Li L. Thermally stable and green cellulose-based composites strengthened by styrene-co-acrylate latex for lithium-ion battery separators. Carbohydr Polym 2019;206:801–10.
[158] Deng J, Cao D, Yang X, Zhang G. Cross-linked cellulose/carboxylated polyimide nanofiber separator for lithium-ion battery application. Chem Eng J 2022;433: 133934.
[159] Liao C, Mu X, Han L, Li Z, Zhu Y, Lu J, Wang H, Song L, Kan Y, Hu Y. A flame-retardant, high ionic-conductivity and eco-friendly separator prepared by papermaking method for high-performance and superior safety lithium-ion batteries. Energy Storage Mater 2022;48:123–32.
[160] Zhang K, Chen H, Huang H, Wei Z, Zhao Y. Water-soluble ammonium polyphosphate synchronously enables mechanically robust and flame-retardant cellulose composite separator for high safety lithium batteries. J Power Sources 2023;558:232627.
[161] Xu Q, Wei C, Fan L, Peng S, Xu W, Xu J. A bacterial cellulose/Al_2O_3 nanofibrous composite membrane for a lithium-ion battery separator. Cellulose 2017;24: 1889–99.
[162] Hu J, Liu Y, Zhang M, He J, Ni P. A separator based on cross-linked nano-SiO_2 and cellulose acetate for lithium-ion batteries. Electrochim Acta 2020;334:135585.
[163] Huang C, Ji H, Guo B, Luo L, Xu W, Li J, Xu J. Composite nanofiber membranes of bacterial cellulose/halloysite nanotubes as lithium ion battery separators. Cellulose 2019;26:6669–81.
[164] Zhang K, Xiao W, Li X, Liu J, Yan C. Highly thermostable expanded polytetrafluoroethylene separator with mussel-inspired silica coating for advanced Li-ion batteries. J Power Sources 2020;468:228403.
[165] Cao C, Tan L, Liu W, Ma J, Li L. Polydopamine coated electrospun poly(vinyldiene fluoride) nanofibrous membrane as separator for lithium-ion batteries. J Power Sources 2014;248:224–9.

[166] Li L, Yu M, Jia C, Liu J, Lv Y, Liu Y, Zhou Y, Liu C, Shao Z. Cellulosic biomass-reinforced polyvinylidene fluoride separators with enhanced dielectric properties and thermal tolerance. ACS Appl Mater Interfaces 2017;9:20885–94.

[167] Wang L, Wang Z, Sun Y, Liang X, Xiang H. Sb_2O_3 modified PVDF-CTFE electrospun fibrous membrane as a safe lithium-ion battery separator. J Membr Sci 2019;572:512–9.

[168] Fang C, Yang S, Zhao X, Du P, Xiong J. Electrospun montmorillonite modified poly(vinylidene fluoride) nanocomposite separators for lithium-ion batteries. Mater Res Bull 2016;79:1–7.

[169] Zhang J, Xiang Y, Jamil MI, Lu J, Zhang Q, Zhan X, Zhan X, Chen F. Polymers/zeolite nanocomposite membranes with enhanced thermal and electrochemical performances for lithium-ion batteries. J Membr Sci 2018;564:753–61.

[170] Tian X, Xin B, Lu Z, Gao W, Zhang F. Electrospun sandwich polysulfonamide/polyacrylonitrile/polysulfonamide composite nanofibrous membranes for lithium-ion batteries. RSC Adv 2019;9:11220–9.

[171] Gao Y, Sang X, Chen Y, Li Y, Liu B, Sheng J, Feng Y, Li L, Liu H, Wang X, Kuang C, Zhai Y. Polydopamine modification electrospun polyacrylonitrile fibrous membrane with decreased pore size and dendrite mitigation for lithium ion battery. J Mater Sci 2020;55:3549–60.

[172] Yanilmaz M, Lu Y, Zhu J, Zhang X. Silica/polyacrylonitrile hybrid nanofiber membrane separators via sol-gel and electrospinning techniques for lithium-ion batteries. J Power Sources 2016;313:205–12.

[173] Liang X, Yang Y, Jin X, Cheng J. Polyethylene oxide-coated electrospun polyimide fibrous seperator for high-performance lithium-ion battery. J Mater Sci Technol 2016;32:200–6.

[174] Wang Y, Wang S, Fang J, Ding LX, Wang H. A nano-silica modified polyimide nanofiber separator with enhanced thermal and wetting properties for high safety lithium-ion batteries. J Membr Sci 2017;537:248–54.

[175] Zhai Y, Xiao K, Yu J, Ding B. Closely packed x-poly(ethylene glycol diacrylate) coated polyetherimide/poly(vinylidene fluoride) fiber separators for lithium ion batteries with enhanced thermostability and improved electrolyte wettability. J Power Sources 2016;325:292–300.

[176] Li H, Zhang B, Liu W, Lin B, Ou Q, Wang H, Fang M, Liu D, Neelakandan S, Wang L. Effects of an electrospun fluorinated poly(ether ether ketone) separator on the enhanced safety and electrochemical properties of lithium ion batteries. Electrochim Acta 2018;290:150–64.

[177] Xiong M, Tang H, Wang Y, Lin Y, Sun M, Yin Z, Pan M. Expanded polytetrafluoroethylene reinforced polyvinylidenefluoride–hexafluoropropylene separator with high thermal stability for lithium-ion batteries. J Power Sources 2013;241:203–11.

[178] Xu H, Li D, Liu Y, Jiang Y, Li F, Xue B. Preparation of halloysite/polyvinylidene fluoride composite membrane by phase inversion method for lithium ion battery. J Alloys Compd 2019;790:305–15.

[179] Gao Z, Luo L, Wen R, Song X, Gao Z, Zheng Z, Zhang J. A multifunctional composite membrane for high-safety lithium-ion batteries. J Mater Chem A 2023;11:1774–84.

[180] Yuan B, Liu J, Dong L, Chen D, Zhong S, Liang Y, Liu Y, Ji Y, Wu X, Kong Q, Han J, He W. A single-layer composite separator with 3D-reinforced microstructure for practical high-temperature lithium ion batteries. Small 2022;18:2107664.

[181] Liu C, Shao Z, Wang J, Lu C, Wang Z. Eco-friendly polyvinyl alcohol/cellulose nanofiber–Li^+ composite separator for high-performance lithium-ion batteries. RSC Adv 2016;6:97912–20.

[182] Xia Y, Li X, Zhuang J, Yuan Y, Wang W. Cellulose microspheres enhanced polyvinyl alcohol separator for high-performance lithium-ion batteries. Carbohydr Polym 2023;300:120231.

[183] Zhang C, Shen L, Shen J, Liu F, Chen G, Tao R, Ma S, Peng Y, Lu Y. Anion-sorbent composite separators for high-rate lithium-ion batteries. Adv Mater 2019;31:1808338.

[184] Kim YJ, Kim HS, Doh CH, Kim SH, Lee SM. Technological potential and issues of polyacrylonitrile based nanofiber non-woven separator for Li-ion rechargeable batteries. J Power Sources 2013;244:196–206.

[185] Evans T, Lee JH, Bhat V, Lee SH. Electrospun polyacrylonitrile microfiber separators for ionic liquid electrolytes in Li-ion batteries. J Power Sources 2015;292:1–6.

[186] Zhao M, Wang J, Chong C, Yu X, Wang L, Shi Z. An electrospun lignin/polyacrylonitrile nonwoven composite separator with high porosity and thermal stability for lithium-ion batteries. RSC Adv 2015;5:101115–20.

[187] Yusuf A, Avvaru VS, Dirican M, Changchun S, Wang DY. Low heat yielding electrospun phosphenanthrene oxide loaded polyacrylonitrile composite separators for safer high energy density lithium-ion batteries. Appl Mater Today 2020;20:100675.

[188] He C, Liu J, Li J, Zhu F, Zhao H. Blending based polyacrylonitrile/poly(vinyl alcohol) membrane for rechargeable lithium ion batteries. J Membr Sci 2018;560:30–7.

[189] Guo M, Xiong J, Jin X, Lu S, Zhang Y, Xu J, Fan H. Mussel stimulated modification of flexible Janus PAN/PVDF-HFP nanofiber hybrid membrane for advanced lithium-ion batteries separator. J Membr Sci 2023;675:121533.

[190] Leng X, Yang M, Li C, Wu Arifeen, Ko TJ. High-performance separator for lithium-ion battery based on dual-hybridizing of materials and processes. Chem Eng J 2022;433:133773.

[191] Wang Q, Song WL, Fan LZ, Song Y. Facile fabrication of polyacrylonitrile/alumina composite membranes based on triethylene glycol diacetate-2-propenoic acid butyl ester gel polymer electrolytes for high-voltage lithium-ion batteries. J Membr Sci 2015;486:21–8.

[192] Liang Y, Ji L, Guo B, Lin Z, Yao Y, Li Y, Alcoutlabi M, Qiu Y, Zhang X. Preparation and electrochemical characterization of ionic-conducting lithium lanthanum titanate oxide/polyacrylonitrile submicron composite fiber-based lithium-ion battery separators. J Power Sources 2011;196:436–41.

[193] Cho JH, Park JH, Kim JH, Lee SY. Facile fabrication of nanoporous composite separator membranes for lithium-ion batteries: poly(methyl methacrylate) colloidal particles-embedded nonwoven poly(ethylene terephthalate). J Mater Chem 2011;21:8192–8.

[194] Jeong HS, Kim JH, Lee SY. A novel poly(vinylidene fluoride-hexafluoropropylene)/poly(ethylene terephthalate) composite nonwoven separator with phase inversion-controlled microporous structure for a lithium-ion battery. J Mater Chem 2010;20:9180–6.

[195] Ding J, Kong Y, Li P, Yang J. Polyimide/Poly(ethylene terephthalate) composite membrane by electrospinning for nonwoven separator for lithium-ion battery. J Electrochem Soc 2012;159:A1474–80.

[196] Choi ES, Lee SY. Particle size-dependent, tunable porous structure of a SiO_2/poly(vinylidene fluoride-hexafluoropropylene)-coated poly(ethylene terephthalate) nonwoven composite separator for a lithium-ion battery. J Mater Chem 2011;21:14747–54.

[197] Liu Q, Xia M, Chen J, Tao Y, Wang Y, Liu K, Li M, Wang W, Wang D. High performance hybrid Al_2O_3/poly(vinyl alcohol-co-ethylene) nanofibrous membrane for lithium-ion battery separator. Electrochim Acta 2015;176:949–55.

[198] Zhu C, Nagaishi T, Shi J, Lee H, Wong PY, Sui J, Hyodo K, Kim IS. Enhanced wettability and thermal stability of a novel polyethylene terephthalate-based poly (vinylidene fluoride) nanofiber hybrid membrane for the separator of lithium-ion batteries. ACS Appl Mater Interfaces 2017;9:26400–6.

[199] Zhang H, Lin CE, Zhou MY, John AE, Zhu BK. High thermal resistance polyimide separators prepared via soluble precusor and non-solvent induced phase separation process for lithium ion batteries. Electrochim Acta 2016;187:125–33.

[200] Li M, Zhang Z, Yin Y, Guo W, Bai Y, Zhang F, Zhao B, Shen F, Han X. Novel polyimide separator prepared with two porogens for safe lithium-ion batteries. ACS Appl Mater Interfaces 2020;12:3610–6.

[201] Deng Y, Pan Y, Zhang Z, Fu Y, Gong L, Liu C, Yang J, Zhang H, Cheng X. Novel thermotolerant and flexible polyimide aerogel separator achieving advanced lithium-ion batteries. Adv Funct Mater 2022;32:2106176.

[202] Wang Y, Guo M, Fu H, Wu Z, Zhang Y, Chao G, Chen S, Zheng L, Liu T. Thermotolerant separator of cross-linked polyimide fibers with narrowed pore size for lithium-ion batteries. J Membr Sci 2022;662:121004.

[203] Sun G, Jiang S, Feng X, Shi X, Zhang X, Li T, Chen N, Hou L, Qi S, Wu D. Ultra-robust polyimide nanofiber separators with shutdown function for advanced lithium-ion batteries. J Membr Sci 2022;645:120208.

[204] Shi J, Shen T, Hu H, Xia Y, Liu Z. Sandwich-like heat-resistance composite separators with tunable pore structure for high power high safety lithium ion batteries. J Power Sources 2014;271:134–42.

[205] Kong L, Yan Y, Qiu Z, Zhou Z, Hu J. Robust fluorinated polyimide nanofibers membrane for high-performance lithium-ion batteries. J Membr Sci 2018;549:321–31.

[206] Sun G, Kong L, Liu B, Niu H, Zhang M, Tian G, Qi S, Wu D. Ultrahigh-strength, nonflammable and high-wettability separators based on novel polyimide-core@polybenzimidazole-sheath nanofibers for advanced and safe lithium-ion batteries. J Membr Sci 2019;582:132–9.

[207] Cho W, Kim SM, Song JH, Yim T, Woo SG, Lee KW, Kim JS, Kim YJ. Improved electrochemical and thermal properties of nickel rich $LiNi_{0.6}Co_{0.2}Mn_{0.2}O_2$ cathode materials by SiO_2 coating. J Power Sources 2015;282:45–50.

[208] Lee J, Lee CL, Park K, Kim ID. Synthesis of an Al_2O_3-coated polyimide nanofiber mat and its electrochemical characteristics as a separator for lithium ion batteries. J Power Sources 2014;248:1211–7.

[209] Dong G, Liu B, Sun G, Tian G, Qi S, Wu D. TiO_2 nanoshell@polyimide nanofiber membrane prepared via a surface-alkaline-etching and in-situ complexation-hydrolysis strategy for advanced and safe LIB separator. J Membr Sci 2019;577:249–57.

[210] Li X, Liu K, Yan Y, Yu J, Dong N, Liu B, Tian G, Qi S, Wu D. Thermostable and nonflammable polyimide/zirconia compound separator for lithium-ion batteries with superior electrochemical and safe properties. J Colloid Interface Sci 2022;625:936–45.

[211] Liao C, Wang W, Wang J, Han L, Qiu S, Song L, Gui Z, Kan Y, Hu Y. Magnetron sputtering deposition of silicon nitride on polyimide separator for high-temperature lithium-ion batteries. J Energy Chem 2021;56:1–10.

[212] Li D, Zhang H, Li X. Porous polyetherimide membranes with tunable morphology for lithium-ion battery. J Membr Sci 2018;565:42–9.

[213] l'Abee R, DaRosa F, Armstrong MJ, Hantel MM, Mourzagh D. High temperature stable Li-ion battery separators based on polyetherimides with improved electrolyte compatibility. J Power Sources 2017;345:202–11.

[214] Wang H, Zhang S, Zhu M, Sui G, Yang X. Remarkable heat-resistant halloysite nanotube/polyetherimide composite nanofiber membranes for high performance gel polymer electrolyte in lithium ion batteries. J Electroanal Chem 2018;808:303–10.

[215] Zhai Y, Xiao K, Yu J, Yang J, Ding B. Thermostable and nonflammable silica–polyetherimide–polyurethane nanofibrous separators for high power lithium ion batteries. J Mater Chem A 2015;3:10551–8.

[216] Li H, Zhang B, Lin B, Yang Y, Zhao Y, Wang L. Electrospun poly(ether ether ketone) nanofibrous separator with superior performance for lithium-ion batteries. J Electrochem Soc 2018;165:A939–46.

[217] Li J, Niu X, Song J, Li Y, Li X, Hao W, Fang J, He T. Harvesting vapor by hygroscopic acid to create pore: morphology, crystallinity and performance of poly (ether ether ketone) lithium ion battery separator. J Membr Sci 2019;577:1–11.

[218] Liu J, Mo Y, Wang S, Ren S, Han D, Xiao M, Sun L, Meng Y. Ultrastrong and heat-resistant poly(ether ether ketone) separator for dendrite-proof and heat-resistant lithium-ion batteries. ACS Appl Energy Mater 2019;2:3886–95.

[219] Le Mong A, Kim D. Tailor-made pore controlled poly (arylene ether ketone) membranes as a lithium-ion battery separator. J Power Sources 2016;304:301–10.

[220] Kim M, Han GY, Yoon KJ, Park JH. Preparation of a trilayer separator and its application to lithium-ion batteries. J Power Sources 2010;195:8302–5.

[221] Liu B, Huang Y, Zhao L, Huang Y, Song A, Lin Y, Wang M, Li X, Cao H. A novel non-woven fabric supported gel polymer electrolyte based on poly (methylmethacrylate-polyhedral oligomeric silsesquioxane) by phase inversion method for lithium ion batteries. J Membr Sci 2018;564:62–72.

[222] Liu X, Zhang B, Wu Y, Chen J, Fang M, Wang L, Wang L. The effects of polybenzimidazole nanofiber separator on the safety and performance of lithium-ion batteries: characterization and analysis from the perspective of mechanism. J Power Sources 2020;475:228624.

[223] Wang J, He Y, Wu Q, Zhang Y, Li Z, Liu Z, Huo S, Dong J, Zeng D, Cheng H. A facile non-solvent induced phase separation process for preparation of highly porous polybenzimidazole separator for lithium metal battery application. Sci Rep 2019;9:19320.

[224] Hao X, Zhu J, Jiang X, Wu H, Qiao J, Sun W, Wang Z, Sun K. Ultrastrong polyoxyzole nanofiber membranes for dendrite-proof and heat-resistant battery separators. Nano Lett 2016;16:2981–7.

[225] Khurana R, Schaefer JL, Archer LA, Coates GW. Suppression of lithium dendrite growth using cross-linked polyethylene/poly(ethylene oxide) electrolytes: a new approach for practical lithium-metal polymer batteries. J Am Chem Soc 2014; 136:7395–402.

[226] Zhao H, Deng N, Yan J, Kang W, Ju J, Wang L, Li Z, Cheng B. Effect of OctaphenylPolyhedral oligomeric silsesquioxane on the electrospun Poly-m-phenylene isophthalamid separators for lithium-ion batteries with high safety and excellent electrochemical performance. Chem Eng J 2019;356:11–21.

[227] Kang W, Deng N, Ma X, Ju J, Li L, Liu X, Cheng B. A thermostability gel polymer electrolyte with electrospun nanofiber separator of organic F-doped poly-m-phenyleneisophthalamide for lithium-ion battery. Electrochim Acta 2016;216: 276–86.

[228] Xiao K, Zhai Y, Yu J, Ding B. Nanonet-structured poly(m-phenylene isophthalamide)–polyurethane membranes with enhanced thermostability and wettability for high power lithium ion batteries. RSC Adv 2015;5:55478–85.

[229] Li Y, Ma X, Deng N, Kang W, Zhao H, Li Z, Cheng B. Electrospun SiO_2/PMIA nanofiber membranes with higher ionic conductivity for high temperature resistance lithium-ion batteries. Fibers Polym 2017;18:212–20.

[230] Yu Y, Jia G, Zhao L, Xiang H, Hu Z, Xu G, Zhu M. Flexible and heat-resistant polyphenylene sulfide ultrafine fiber hybrid separators for high-safety lithium-ion batteries. Chem Eng J 2023;452:139112.

[231] Luo D, Chen M, Xu J, Yin X, Wu J, Chen S, Wang L, Wang H. Polyphenylene sulfide nonwoven-based composite separator with superior heat-resistance and flame retardancy for high power lithium ion battery. Compos Sci Technol 2018; 157:119–25.

[232] Zhu C, Zhang J, Xu J, Yin X, Wu J, Chen S, Zhu Z, Wang L, Wang H. Aramid nanofibers/polyphenylene sulfide nonwoven composite separator fabricated through a facile papermaking method for lithium ion battery. J Membr Sci 2019; 588:117169.

[233] Zhu C, Zhang J, Xu J, Yin X, Wu J, Chen S, Zhu Z, Wang L, Wang H. Facile fabrication of cellulose/polyphenylene sulfide composite separator for lithium-ion batteries. Carbohydr Polym 2020;248:116753.

[234] Woo JJ, Nam SH, Seo SJ, Yun SH, Kim WB, Xu T, Moon SH. A flame retarding separator with improved thermal stability for safe lithium-ion batteries. Electrochem Commun 2013;35:68–71.

[235] Woo JJ, Zhang Z, Dietz Rago NL, Lu W, Amine K. A high performance separator with improved thermal stability for Li-ion batteries. J Mater Chem A 2013;1: 8538–40.

[236] Yang H, Shi X, Chu S, Shao Z, Wang Y. Design of block-copolymer nanoporous membranes for robust and safer lithium-ion battery separators. Adv Sci 2021;8: 2003096.

[237] Hauser RL. Cross-linked, microporous polysulfone battery electrode separator. US. Pat. No. 10522808B2; 2019.

[238] Barbosa JC, Reizabal A, Correia DM, Fidalgo-Marijuan A, Gonçalves R, Silva MM, Mendez SL, Costa CM. Lithium-ion battery separator membranes based on poly(L-lactic acid) biopolymer. Mater Today Energy 2020;18:100494.

[239] Thiangtham S, Saito N, Manuspiya H. Asymmetric porous and highly hydrophilic sulfonated cellulose/biomembrane functioning as a separator in a lithium-ion battery. ACS Appl Energy Mater 2022;5:6206–18.

[240] Laezza A, Celeste A, Curcio M, Teghil R, De Bonis A, Brutti S, Pepe A, Bochicchio B. Cellulose nanocrystals as additives in electrospun biocompatible separators for aprotic lithium-ion batteries. ACS Appl Polym Mater 2023;5: 1453–63.

[241] Zhang Y, Wang Z, Xiang H, Shi P, Wang H. A thin inorganic composite separator for lithium-ion batteries. J Membr Sci 2016;509:19–26.

[242] Liao YH, Li XP, Fu CH, Xu R, Zhou L, Tan CL, Hu SJ, Li WS. Polypropylene-supported and nano-Al_2O_3 doped poly(ethylene oxide)–poly(vinylidene fluoride-hexafluoropropylene)-based gel electrolyte for lithium ion batteries. J Power Sources 2011;196:2115–21.

[243] Xiang H, Chen J, Li Z, Wang H. An inorganic membrane as a separator for lithium-ion battery. J Power Sources 2011;196:8651–5.

[244] Wang Z, Xiang H, Wang L, Xia R, Nie S, Chen C, Wang H. A paper-supported inorganic composite separator for high-safety lithium-ion batteries. J Membr Sci 2018;553:10–6.

[245] Huang X, Hitt J. Lithium ion battery separators: development and performance characterization of a composite membrane. J Membr Sci 2013;425–426:163–8.

[246] Zhang S, Cao J, Shang Y, Wang L, He X, Li J, Zhao P, Wang Y. Nanocomposite polymer membrane derived from nano TiO_2-PMMA and glass fiber nonwoven: high thermal endurance and cycle stability in lithium ion battery applications. J Mater Chem A 2015;3:17697–703.

[247] He M, Zhang X, Jiang K, Wang J, Wang Y. Pure inorganic separator for lithium ion batteries. ACS Appl Mater Interfaces 2015;7:738–42.

[248] Mi W, Sharma G, Dong X, Jin Y, Lin YS. Electrode-supported thin α-alumina separators for lithium-ion batteries. J Power Sources 2016;305:209–16.

[249] Chen P, Shen J, Wang T, Dai M, Si C, Xie J, Li M, Cong X, Sun X. Zeolitic imidazolate framework-67 based separator for enhanced high thermal stability of lithium ion battery. J Power Sources 2018;400:325–32.

[250] Pan R, Cheung O, Wang Z, Tammela P, Huo J, Lindh J, Edstrom K, Stromme M, Nyholm L. Mesoporous Cladophora cellulose separators for lithium-ion batteries. J Power Sources 2016;321:185–92.

[251] Zhang LC, Sun X, Hu Z, Yuan CC, Chen CH. Rice paper as a separator membrane in lithium-ion batteries. J Power Sources 2012;204:149–54.

[252] Gong SD, Huang Y, Cao HJ, Lin YH, Li Y, Tang SH, Wang MS, Li X. A green and environment-friendly gel polymer electrolyte with higher performances based on the natural matrix of lignin. J Power Sources 2016;307:624–33.

[253] Zhang TW, Shen B, Yao HB, Ma T, Lu LL, Zhou F, Yu SH. Prawn shell derived chitin nanofiber membranes as advanced sustainable separators for Li/Na-ion batteries. Nano Lett 2017;17:4894–901.

[254] Pereira RFP, Brito-Pereira R, Gonçalves R, Silva MP, Costa CM, Silva MM, Bermudez VZ, Mendez SL. Silk fibroin separators: a step toward lithium-ion batteries with enhanced sustainability. ACS Appl Mater Interfaces 2018;10: 5385–94.

[255] Li Z, Wang W, Liang X, Wang J, Xu Y, Li W. Fiber swelling to improve cycle performance of paper-based separator for lithium-ion batteries application. J Energy Chem 2023;79:92–100.

[256] Kim DJ, Hermann KR, Prokofjevs A, Otley MT, Pezzato C, Owczarek M, Stoddart JF. Redox-active macrocycles for organic rechargeable batteries. J Am Chem Soc 2017;139:6635–43.

[257] Wang S, Wang Q, Shao P, Han Y, Gao X, Ma L, Yuan S, Ma X, Zhou J, Feng X, Wang B. Exfoliation of covalent organic frameworks into few-layer redox-active nanosheets as cathode materials for lithium-ion batteries. J Am Chem Soc 2017; 139:4258–61.

[258] Mai LQ, Minhas-Khan A, Tian X, Hercule KM, Zhao YL, Lin X, Xu X. Synergistic interaction between redox-active electrolyte and binder-free functionalized carbon for ultrahigh supercapacitor performance. Nat Commun 2013;4:2923.

[259] Hwang C, Lee J, Jeong J, Lee E, Kim J, Kim S, Yang C, Song HK. The rational design of a redox-active mixed ion/electron conductor as a multi-functional binder for lithium-ion batteries. J Mater Chem A 2021;9:4751–7.

[260] Yu J, He Y, Zou S, Na B, Liu H, Liu J, Li H. Redox-active manganese dioxide@ polypropylene hybrid separators for advanced lithium ion batteries. Appl Surf Sci 2020;508:144757.

[261] Wang Z, Pan R, Ruan C, Edström K, Strømme M, Nyholm L. Redox-active separators for lithium-ion batteries. Adv Sci 2018;5:1700663.

[262] Pan R, Wang Z, Sun R, Lindh J, Edström K, Strømme M, Nyholm L. Polydopamine-based redox-active separators for lithium-ion batteries. J. Materiomics. 2019;5: 204–13.

[263] Shi C, Zhang P, Huang S, He X, Yang P, Wu D, Sun D, Zhao J. Functional separator consisted of polyimide nonwoven fabrics and polyethylene coating layer for lithium-ion batteries. J Power Sources 2015;298:158–65.

[264] Kim Y, Lee WY, Kim KJ, Yu JS, Kim YJ. Shutdown-functionalized nonwoven separator with improved thermal and electrochemical properties for lithium-ion batteries. J Power Sources 2016;305:225–32.

[265] Ding L, Yan N, Zhang S, Xu R, Wu T, Yang F, Cao Y, Xiang M. Low-cost mass manufacturing technique for the shutdown-functionalized lithium-ion battery separator based on Al_2O_3 coating online construction during the β-iPP cavitation process. ACS Appl Mater Interfaces 2022;14:6714–28.

[266] Xiao Y, Fu A, Zou Y, Huang L, Wang H, Su Y, Zheng J. High safety lithium-ion battery enabled by a thermal-induced shutdown separator. Chem Eng J 2022;438: 135550.

[267] Wei Z, Gu J, Zhang F, Pan Z, Zhao Y. Core–shell structured nanofibers for lithium ion battery separator with wide shutdown temperature window and stable electrochemical performance. ACS Appl Polym Mater 2020;2:1989–96.

[268] Jiang X, Xiao L, Ai X, Yang H, Cao Y. A novel bifunctional thermo-sensitive poly (lactic acid)@poly(butylene succinate) core–shell fibrous separator prepared by a coaxial electrospinning route for safe lithium-ion batteries. J Mater Chem A 2017; 5:23238–42.

[269] Zainab G, Wang X, Yu J, Zhai Y, Ahmed Babar A, Xiao K, Ding B. Electrospun polyacrylonitrile/polyurethane composite nanofibrous separator with electrochemical performance for high power lithium ion batteries. Mater Chem Phys 2016;182:308–14.

[270] Zhai Y, Wang N, Mao X, Si Y, Yu J, Al-Deyab SS, Newehy M, Ding B. Sandwich-structured PVdF/PMIA/PVdF nanofibrous separators with robust mechanical strength and thermal stability for lithium ion batteries. J Mater Chem A 2014;2: 14511–8.

[271] Li Z, Xiong Y, Sun S, Zhang L, Li S, Liu X, Xu Z, Xu S. Tri-layer nonwoven membrane with shutdown property and high robustness as a high-safety lithium ion battery separator. J Membr Sci 2018;565:50–60.